

Inferring fine-grained migration patterns across the United States

Gabriel Agostini¹, Rachel Young^{2, 3, 4}, Maria Fitzpatrick⁵, Nikhil Garg¹,
Emma Pierson^{3 *}

¹Cornell Tech, New York City, NY, United States.

²University of Minnesota, Minneapolis, MN, United States.

³University of California, Berkeley, Berkeley, CA, United States.

⁴Princeton University, Princeton, NJ, United States.

⁵Cornell University, Ithaca, NY, United States.

***Corresponding author:** emmapierson@berkeley.edu.

Abstract

Fine-grained migration data illuminate demographic, environmental, and health phenomena. However, United States migration data have serious drawbacks: public data lack spatiotemporal granularity, and higher-resolution proprietary data suffer from multiple biases. To address this, we develop a method that fuses high-resolution proprietary data with coarse Census data to create MIGRATE: annual migration matrices capturing flows between 47.4 billion US Census Block Group pairs—approximately four thousand times the spatial resolution of current public data. Our estimates are highly correlated with external ground-truth datasets and improve accuracy relative to raw proprietary data. We use MIGRATE to analyze national and local migration patterns. Nationally, we document demographic and temporal variation in homophily, upward mobility, and moving distance—for example, rising moves into top-income-quartile block groups and racial disparities in upward mobility. Locally, MIGRATE reveals patterns such as wildfire-driven out-migration that are invisible in coarser previous data. We release MIGRATE as a resource for migration researchers.

1 Introduction

Fine-grained migration data, which record the number of people relocating from one geographic area to another, are essential for understanding a range of social, environmental, and health phenomena. Migration data illuminate responses to environmental disasters and climate change^[1–4]; responses to economic stresses and opportunities^[5–8]; patterns of social change^[9]; consequences of conflicts^[10,11]; effects of the COVID-19 pandemic^[12]; housing instability^[13,14]; urban-suburban migration patterns^[15,16]; and political polarization^[17].

But migration datasets within the United States have serious limitations. The most fine-grained publicly available national datasets track migration at the county level^[18]. While widely used, these datasets lack sufficient spatial resolution to study a number of phenomena where previous research has revealed important variation at the sub-county level. For example, research on flood-risk-induced migration uses models at the much more granular Census block level^[19], arguing that this spatial granularity is necessary due to the highly localized nature of flood risk^[20]. Other research on climate-induced vulnerability, eviction or displacement similarly models risk at a sub-county (Census tract) level^[14,21] or even at the household level^[22]. Research on housing instability often models Census Block Groups^[23] or even specific building complexes^[24]. All of these applications testify to the need for highly granular data to facilitate accurate study of many important migration-related phenomena.

Additionally, movers within the same county have accounted for more than half of migratory flows in the United States in all years from 2006 to 2019^[25]. Publicly available, county-level migration datasets are too coarse to study these important migration patterns.

Proprietary migration datasets offer greater granularity. Data aggregators like Infutor^[26] combine many data sources — including voter files, property deeds, credit files, and phone books^[27–29] — to attempt to infer address histories for individual-level movers. Such datasets have been widely used because they are extremely temporally and spatially fine-grained^[5,13,28,30–32]. A long literature which provides more recent or granular migration estimates using non-traditional data sources, including social media and digital advertisement data, testifies to the power of new data sources^[4,10,11,33,34]. Previous work also suggests that address history data do contain valuable signal which correlates with external datasets, as validated by cross-referencing the data with hurricanes or public housing foreclosures^[13], and with marginal population counts in the region of interest^[27]. However, proprietary address history datasets have three major disadvantages. First, they are not publicly available, limiting their utility to researchers. Second, they require extensive computational pipelines, and substantial computational resources, to clean and map to standardized geographical areas to facilitate subsequent analysis. Third, and most fundamentally, they combine multiple imperfect data sources using proprietary algorithms, and thus contain noise and biases. For example, Infutor and other consumer record datasets have been shown to overrepresent higher-income and majority-group populations in some settings^[35].

To address the limitations of existing migration data, we create and release **MIGRATE** (**M**igration **I**nference for **GR**Anular **T**rend **E**stimation): fine-grained migration estimates that combine the strengths of both aforementioned types of data by harmonizing biased but fine-grained proprietary data with reliable but coarse Census data. To produce our estimates, we develop a data fusion method^[36,37] based on iterative proportional fitting (IPF)^[38–40] to reconcile the raw migration data from data aggregator Infutor with the more reliable Census constraints. The output of our method is a set of yearly inferred United States migration matrices at the Census Block Group (CBG) level from 2010-2019. Our matrices capture migration flows between 47.4 billion pairs of CBGs, making **MIGRATE** approximately 4,600 times more granular than the county-county flows publicly available on the 5-year level, and 18 million times more granular than the state-state flows publicly available on the 1-year level. We comprehensively validate **MIGRATE** by comparing to external data sources, showing that it correlates well with ground-truth population counts and migration flows, and improves accuracy and reduces demographic bias compared to raw Infutor data, which overcounts rural, older, white, and home-owning populations. We then use **MIGRATE** to analyze both national and local

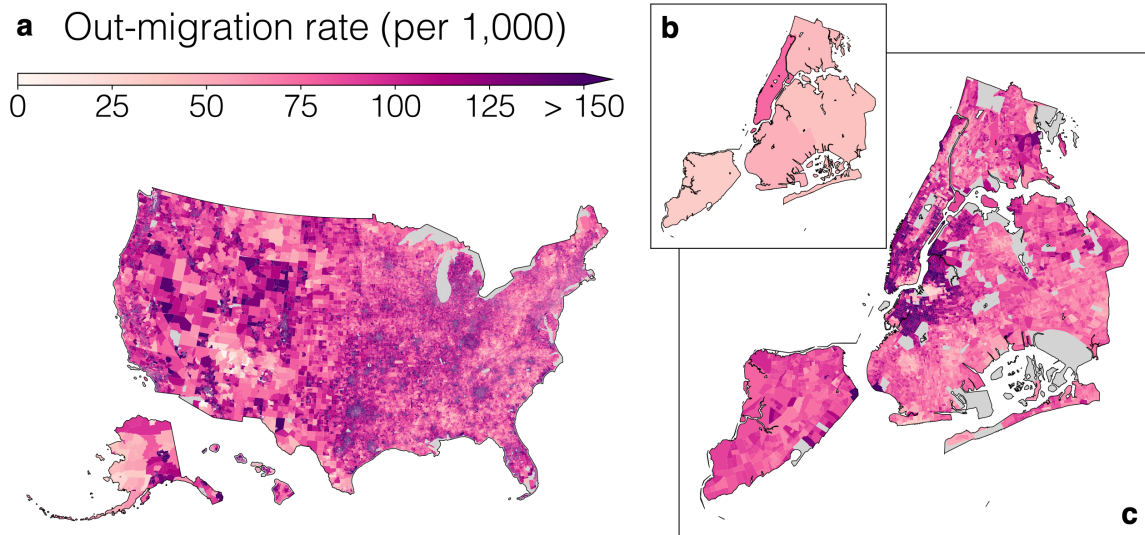


Fig. 1: MIGRATE estimates. We estimate annual migration flows between all pairs of Census block groups (CBGs) from 2010-2019. **(a)** Average MIGRATE estimates of out-migration rates across the entire United States. **(b-c)** MIGRATE estimates of out-migration rates within New York City. MIGRATE estimates reveal granular spatial patterns invisible in publicly available county-to-county data (inset plot **(b)**). Out-migration rates for CBGs with fewer than 100 people are omitted.

migration. Nationally, we reveal both temporal and demographic variation in migration homophily, upward mobility, and moving distance. We find, for example, that people are increasingly likely to move to top-income-quartile CBGs, but also provide evidence of racial disparities: movers from plurality Black CBGs are less likely, and movers from plurality Asian CBGs more likely, to move to top-income-quartile CBGs, and these disparities persist even when controlling for income of origin CBG. Locally, we show that MIGRATE can illuminate important migration patterns, including dramatic increases in out-migration in response to California wildfires, that are invisible in county-level data. To provide a foundation for more precise migration research in the social, environmental, urban, and health sciences, we release MIGRATE for non-profit research use at migrate.tech.cornell.edu.

2 Creating MIGRATE

Here we provide a high-level summary of our method for inferring fine-grained migration matrices by harmonizing Census and Infutor data. In the Methods Section, we provide full details of processing the Infutor dataset (§M.1), processing Census data (§M.2), and harmonizing both data sources (§M.3).

2.1 Preprocessing the raw Infutor dataset

We first preprocess the raw Infutor data into yearly migration matrices. The raw Infutor data consists of sequences of addresses for individual people¹. We use these address sequences to compute the number of people moving between each pair of geographic areas. In particular, we estimate the matrices $E^{(t)}$, where entries $E_{ij}^{(t)}$ represent the number of people who reside in CBG j some time during year t and resided in CBG i a year prior.

We provide a conceptual overview of the preprocessing pipeline here and full details in the Methods Section M.1. We first construct cleaned monthly address histories for each individual in the Infutor dataset by reconciling inconsistencies in address start/end dates, discarding unreliable records (e.g., postal boxes), and modeling uncertainty when multiple addresses are active. These monthly address distributions are then aggregated in a way that simulates ACS survey responses about residence one year prior, producing annual migration flow estimates between pairs of addresses. Finally, to convert the address-address migration matrices to CBG-CBG migration matrices, each address is mapped to one or more CBGs. When the raw Infutor data contains a precise street address (90.40% of all addresses in the dataset), we map each address to a unique 2010 CBG with a state-of-the-art geocoder^[42,43]. We obtain matches for 92.18% of these addresses and confirm by hand inspection of 200 addresses that this yields highly accurate results. The remaining addresses are incomplete or imprecise (e.g., contain only ZIP codes); we probabilistically map these addresses to multiple CBGs, with the weight of each CBG proportional to the population in the CBG intersecting the ZIP code. We are able to map 99.21% of all addresses in Infutor to CBGs. The final output of this preprocessing procedure is the Infutor yearly migration matrices $E^{(t)}$, which capture migration counts between pairs of CBGs as estimated from Infutor data alone. We provide summary statistics for the raw Infutor data and the processed migration matrices for the 2010-2019 time period in Table 1 and additional descriptive statistics in Table 2.

2.2 Harmonizing the Infutor and Census datasets

Having produced the raw Infutor yearly migration matrices $E^{(t)}$, we next reconcile them with more reliable but less granular Census data by rescaling selected entries of $E^{(t)}$. We rescale to different Census datasets in sequence, rather than simultaneously, because the datasets are not totally consistent with each other. Specifically, we first rescale the entries of $E^{(t)}$ to match CBG populations from the Census and 5-year American Community Survey (ACS); then the 1-year ACS counts of movers and non-movers by state; then the 1-year ACS state-to-state flows; and finally the 1-year county populations from the Population Estimates Program (PEP).

The motivation for this ordering is that the 1-year county populations are more precisely estimated than the other datasets, and we thus prioritize matching to them. While CBG populations and state flows are estimated by the ACS and often contain large sampling errors (see our discussion

¹For a subset of individuals, Infutor also provides estimated demographic information (e.g., age, gender, and socioeconomic information). We do not incorporate this information in our analysis for two reasons: first, complete demographic data is only available for about half of all individuals; second, the reliability of estimated demographic information is concerning—as the data lacks documentation, we should not discard the possibility that demographic information has been imputed based on addresses—and contains known and potential biases^[35,41]. Analogously, we do not use Census information on demographic subgroups when harmonizing with Census data; we only make use of population counts and flows.

Individuals with active records (any time in 2010-2019)	374,217,253
Individuals with active records in a given year (average across 2010-2019)	231,270,602
US population in 2010	309,327,143
US population in 2019	328,329,953
Address records per active individual (mean)	2.67
Address records per active individual (median)	2

Table 1: Summary statistics for raw Infutor data and Census data (2010-2019). We define “individuals with active records” as those whose [earliest Infutor date observed, latest Infutor date observed] interval intersects a given time period. Comparing the average yearly number of active individuals in the Infutor data to the Census population (second row) shows that Infutor under-counts the population. (Table 2 provides the number of active individuals in each year from 2010-2019). Active individuals have on average between two and three addresses, translating to one or two moves during the decade.

in Methods Section M.2), county populations are estimated by PEP using more precise large-scale administrative datasets. We verify that incorporating each of these datasets improves our performance on the validations discussed below, and that the performance is not overly sensitive to the order in which we match to the datasets (see Supplementary Table A1).

To perform the final rescaling (matching 1-year county populations) we apply an iterative procedure based on the classical IPF algorithm^[38,39]: specifically, we scale blocks of rows and columns to agree with the annual county populations in years $t - 1$ and t , respectively, alternating between scaling rows and scaling columns until the procedure converges. Only the final rescaling is performed using full IPF; the other rescalings, to CBG populations, 1-year counts of movers and non-movers, and 1-year state-to-state flows, are performed only once at the beginning of the process, as opposed to iteratively, to avoid overfitting to these more noisily estimated datasets. The resulting migration matrices constitute our MIGRATE estimates. In Methods Section M.3, we provide additional details on these scalings.

Naive implementations of our harmonization algorithm impose prohibitive computation times due to the size of the matrices involved. We rely on the sparsity of the problem to dramatically reduce both memory and time requirements, allowing our procedure to converge within 2 hours using 16G of memory and 8 cores. Our general approach — i.e., rescaling submatrices to match Census constraints — can straightforwardly be adapted to accommodate other sources of Census data.

Figure 1 depicts the MIGRATE estimates. Figure 1a plots the average out-migration rates for all CBGs in the United States in the 2010-19 period, highlighting the spatial granularity of the estimates. This granularity often reveals important patterns which are invisible at the county-county level, as we illustrate by zooming in on New York City and comparing the county-level rates obtained from ACS flows (Figure 1b) to the CBG-level out-migration rates inferred by MIGRATE (Figure 1c).

3 Validating MIGRATE

We conduct extensive validations of the MIGRATE estimates. We first show that MIGRATE estimates are highly concordant with Census datasets and improve agreement relative to raw Infutor data (Figure 2). We then investigate demographic biases in the raw Infutor estimates and show that MIGRATE reduces them (Figure 3). In Appendix A.2 we further verify, with experiments on semi-synthetic data, that our method recovers ground-truth flows under certain conditions of bias and noise.

3.1 MIGRATE estimates are highly correlated with ground-truth Census data

MIGRATE estimates are well-correlated with all available Census measures of population counts and flows (Figure 2a-c). By design, MIGRATE estimates perfectly match state and county populations (because the last step in our harmonization procedure is to match to county populations). MIGRATE estimates also achieve Pearson correlation $\rho = 0.997$ with 5-year Census tract populations, and $\rho = 0.996$ with 5-year CBG populations (Figure 2a)². MIGRATE estimates of the number of movers between each pair of states and each pair of counties are also highly correlated with ACS estimates

²To compare our one-year MIGRATE estimates to five-year ACS estimates, we average our estimates across the same periods for consistency with the ACS data, using only ACS data products whose time period completely overlaps with the 2010-2019 MIGRATE range.

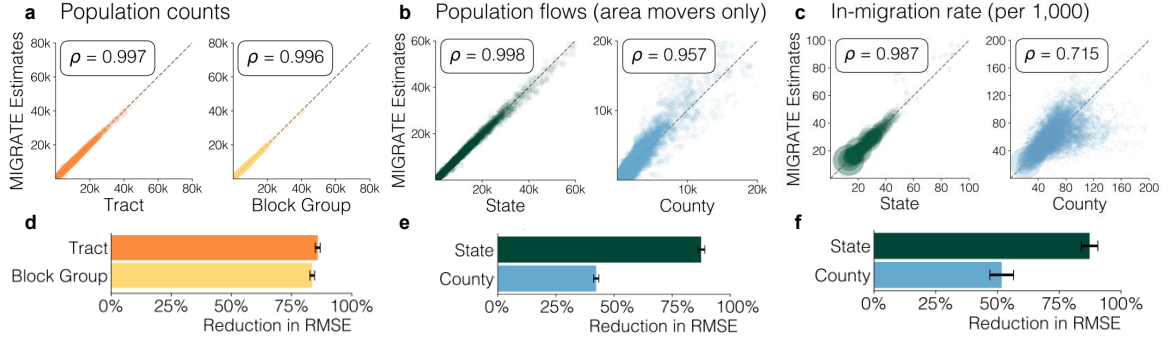


Fig. 2: Validating the MIGRATE estimates. (a - c): MIGRATE estimates (y-axis) are highly correlated with Census data (x-axis), including (a) Census populations at the tract, and block group (CBG) level, (b) movers between each pair of states and each pair of counties (excluding people who remain within the same state or county), and (c) state and county in-migration rates (i.e., the number of people moving into an area as a fraction of the area’s population). For in-migration rates, correlations are weighted by state or county population, and points are sized by population. (d - f) MIGRATE estimates increase agreement with Census datasets relative to raw Infutor data for population counts, movers between states and counties, and in-migration rate, respectively. We compute root mean squared error (RMSE) between (1) MIGRATE estimates and Census data and (2) Infutor data and Census data, and report the reduction in RMSE from using MIGRATE estimates. Bars show the mean reduction in RMSE across all data release years ($n = 5$ for population and county-level migration datasets, $n = 9$ for state-level migration datasets); error bars plot standard deviation across years. For the in-migration rates, RMSE is weighted by area population.

($\rho = 0.998$ and 0.957 for states and counties respectively; Figure 2b)³. Finally, MIGRATE estimates of state and county in-migration rates (i.e., the number of people moving into an area as a fraction of the area’s population) are well-correlated with ACS estimates (Figure 2c; $\rho = 0.987$ and 0.715 for state and county in-migration rates, respectively, weighting by area population). Supplementary Table A1a reports correlations with additional Census quantities (e.g., in-migration counts as opposed to rates) which remain high.

Overall, these validations demonstrate that MIGRATE estimates are highly correlated with ground-truth Census data. This is not merely because of variation in state or county populations, since it remains true when examining in-migration rates, which normalize for population, as well as when looking at tracts and CBGs, which do not vary as significantly in population. Nor is it due merely to the fact that most people do not move, since we examine correlations for movers specifically, as well as correlations with in-migration rates. Finally, it is not merely a consequence of overfitting to Census data, because it remains true on held-out datasets that are not used in our harmonization procedure, a standard check for statistical estimation methods^[44]⁴. Specifically, MIGRATE estimates remain highly correlated with county-county mover counts and county in-migration rates, which are not used in our estimation procedure. As a further held-out validation, we verify that our estimation procedure yields highly correlated estimates with each Census data source even when we remove it from the datasets used for estimation. For example, we remove CBG-level Census populations from our estimation datasets, and verify that our resulting estimates remain highly correlated with data below county level ($\rho = 0.888$ with Census Tract populations and $\rho = 0.856$ with Census Block Group populations). See Supplementary Table A1a for full results.

3.2 MIGRATE estimates reduce error relative to raw Infutor data

We show that MIGRATE estimates also increase agreement with Census datasets compared to using the Infutor data alone. We note that Infutor systematically undercounts the population, as shown in Table 1; to compare to Infutor as generously as possible, and in particular to ensure that MIGRATE does not reduce error due to trivial rescalings, we multiply each raw Infutor matrix $E^{(t)}$ by a scaling

³We exclude people who remain within the same state or county from this calculation, because most people do not move, which artificially inflates the correlation. Supplementary Table 3b reports the correlation without this exclusion, which is nearly perfect.

⁴Even for some Census datasets that are used in our harmonization procedure, we would expect correlations with MIGRATE to be high but not perfect, because the Census datasets are not totally consistent with each other.

factor so it matches the national yearly Census population prior to conducting these comparisons. Figures 2d-f report the reduction in error that MIGRATE estimates achieve relative to Infutor data. We compute root mean squared error (RMSE) between (1) MIGRATE estimates and ground-truth Census data and (2) Infutor data and ground-truth Census data, and report the reduction in RMSE from using MIGRATE estimates. We report average reduction in RMSE across all data releases between 2010 and 2019; error bars represent standard deviation across these releases.

MIGRATE estimates eliminate error in state and county populations because they are constructed to match county-level estimates. They also reduce error in Census Tract and CBG populations by an average of 85.9% and 83.6% respectively (Figure 2d); in state-to-state movers and county-to-county movers by 87.5% and 42.3% (Figure 2e); and in state in-migration and county in-migration rates by 87.3% and 51.8% (Figure 2f). These gains persist even when using held-out datasets that are not used in estimating MIGRATE (namely, county-to-county flows and county in-migration rates). We also repeat the validation above where we successively remove types of data (e.g., CBG-level populations) from our estimation procedure, and verify that our estimation procedure still reduces error in reproducing those held-out data types (Supplementary Table A1b).

Collectively, these validations demonstrate that MIGRATE estimates increase agreement with Census datasets, including held-out datasets, compared to raw Infutor data. We provide error reductions for additional metrics (all flows, non-movers, and in-migration counts as opposed to rates) in Supplementary Table A1b, and conduct additional validations on synthetic data (Appendix A.2).

3.3 MIGRATE estimates reduce demographic biases present in raw Infutor data

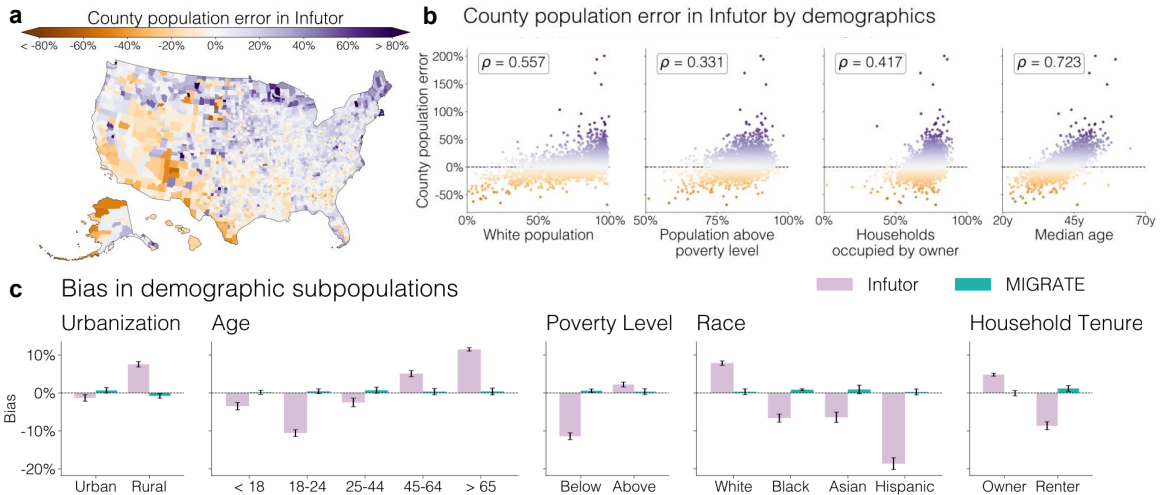


Fig. 3: Assessment of demographic bias in the raw Infutor data and the MIGRATE estimates. Infutor data displays biases that MIGRATE estimates greatly reduce. (a) Average errors in county populations in Infutor data relative to Census data; orange denotes counties where Infutor underrepresents the population, and purple denotes counties where Infutor overrepresents it. MIGRATE estimates remove all county-level errors by construction. (b) Spearman correlation between county demographics (x-axis) and error in Infutor estimates (y-axis). Infutor’s error is correlated with racial, socioeconomic, and other demographic characteristics. (c) Comparison of demographic bias in Infutor (purple) and MIGRATE (green). Bars compare demographic subpopulations estimated from Infutor or MIGRATE to ground-truth Census data, averaged over $n = 5$ population data releases (American Community Survey 5-year estimates, 2015 through 2018) Error bars represent standard deviations across these releases. MIGRATE greatly reduces biases for all demographic subgroups.

The Infutor data displays geographic and demographic biases (Figure 3). Specifically, it overrepresents populations in the counties in the northeastern United States while underrepresenting populations in the southwest (Figure 3a)⁵. Errors plotted are averages of county population errors

⁵For this analysis, as above, we multiply each Infutor matrix $E^{(t)}$ by a scaling factor so it matches the national yearly Census population to avoid deviations due to trivial rescalings.

across all 10 years of data from 2010-2019. MIGRATE estimates remove all such county-level errors by construction.

Errors in the Infutor data also correlate with demographics (Figure 3b). Infutor data overrepresents White, home-owning, richer, and older populations: there is a positive Spearman correlation between the relative error in county population estimates and the population share of a county in each of these groups. These biases are consistent with biases found in previous research^[35], as we discuss in detail in Appendix A.3, and could propagate into biases in downstream analyses of inequality and other topics.

MIGRATE estimates reduce biases in Infutor data. Figure 3c compares the demographic biases of the MIGRATE estimates to the biases of the Infutor data. To quantify bias, we compare (1) the ground-truth number of people within each group (from Census data) to (2) the number of people within each group estimated from Infutor or MIGRATE, which we compute as $\sum_i p_i \cdot n_i$, where i indexes CBGs, p_i is the proportion of people in a CBG within a given group (e.g., the proportion of Black residents) based on Census data, and n_i is the number of people in a CBG in Infutor or MIGRATE. This quantifies how much Infutor and MIGRATE overcount or undercount a given demographic group, relative to ground-truth Census data. The raw Infutor data substantially overcounts rural, older, white, and home-owning populations, and undercounts younger, Black, Asian, Hispanic, renter, and below-the-poverty-line populations; the MIGRATE estimates almost entirely eliminate these biases. We present analyses for additional demographic groups, including immigrant populations, in Appendix A.4.

4 Analysis of national migration patterns

We use MIGRATE to analyze national patterns of migration from 2010-2019. The spatial granularity of the data affords an opportunity to study demographic variation in migration patterns — for example, differences in migration between higher-income and lower-income CBGs — that may be obscured by county or state-level data, which show far less demographic variation. We hence divide CBGs into 10 (overlapping) categories — plurality white, Asian, Black, and Hispanic; urban versus rural; and bottom, second, third, and top income quartile — and stratify the migration statistics we compute by these ten categories. To determine the category of each CBG every year, we use the most recent ACS 5-year demographic estimates. For example, to classify CBGs by their plurality race group to study moves in the 2010-2011 period, we use the ACS 2006-2010 race and ethnicity estimates.

Figure 4a plots flows between the ten categories — for example, the proportion of movers from top-income-quartile CBGs who move to top-income-quartile CBGs. This reveals substantial homophily in migration: out-movers from all ten CBG categories are more likely than movers as a whole to move to CBGs of the same category. However, the strength of this homophily varies across categories. Movers from plurality Black, Asian, and Hispanic CBGs exhibit strong homophily: they are $5.5\times$, $14.6\times$, and $4.3\times$ likelier than movers as a whole to move to CBGs with the same plurality race group (Supplementary Figure B1a reports relative rates for all groups). We also observe income homophily, particularly for movers within top and bottom quartile CBGs: movers from bottom-income-quartile CBGs are nearly twice as likely as movers as a whole to move to CBGs in the bottom income quartile (34% versus 18% for movers as a whole); movers from top-income-quartile CBGs are $1.7\times$ likelier than movers as a whole to move to top-income-quartile CBGs (53% versus 32%). In Supplementary Figure B1b, we confirm that this homophily does not occur merely because many moves are local and demographics are spatially correlated: we also observe homophily when restricting to long-distance (out-of-county) moves.

Figure 4a also shows that people are likelier to move to CBGs in higher income quartiles: 32% of moves are to top-income-quartile CBGs, while only 18% are to bottom-income-quartile CBGs. This trend becomes more pronounced over the decade we study (Supplementary Figure B2d) and is only partially explained by the fact that top-income-quartile CBGs account for a larger share of the population (29%) than bottom-income-quartile CBGs (21%). There are also racial disparities: movers from plurality Asian CBGs are $1.7\times$ likelier than movers as a whole to move to top-income-quartile CBGs; movers from plurality Black CBGs are $2.0\times$ likelier than movers as a whole to move to bottom-income-quartile CBGs.

Figure 4b investigates whether these racial disparities persist when controlling for origin CBG median income: in particular, plotting the share of movers moving to a higher-income CBG when controlling for the mover’s origin CBG median income decile. This reveals that the probability of moving to a higher-income CBG varies substantially by race even conditional on origin CBG income: movers from plurality Asian CBGs are more likely than movers as a whole, and movers from plurality

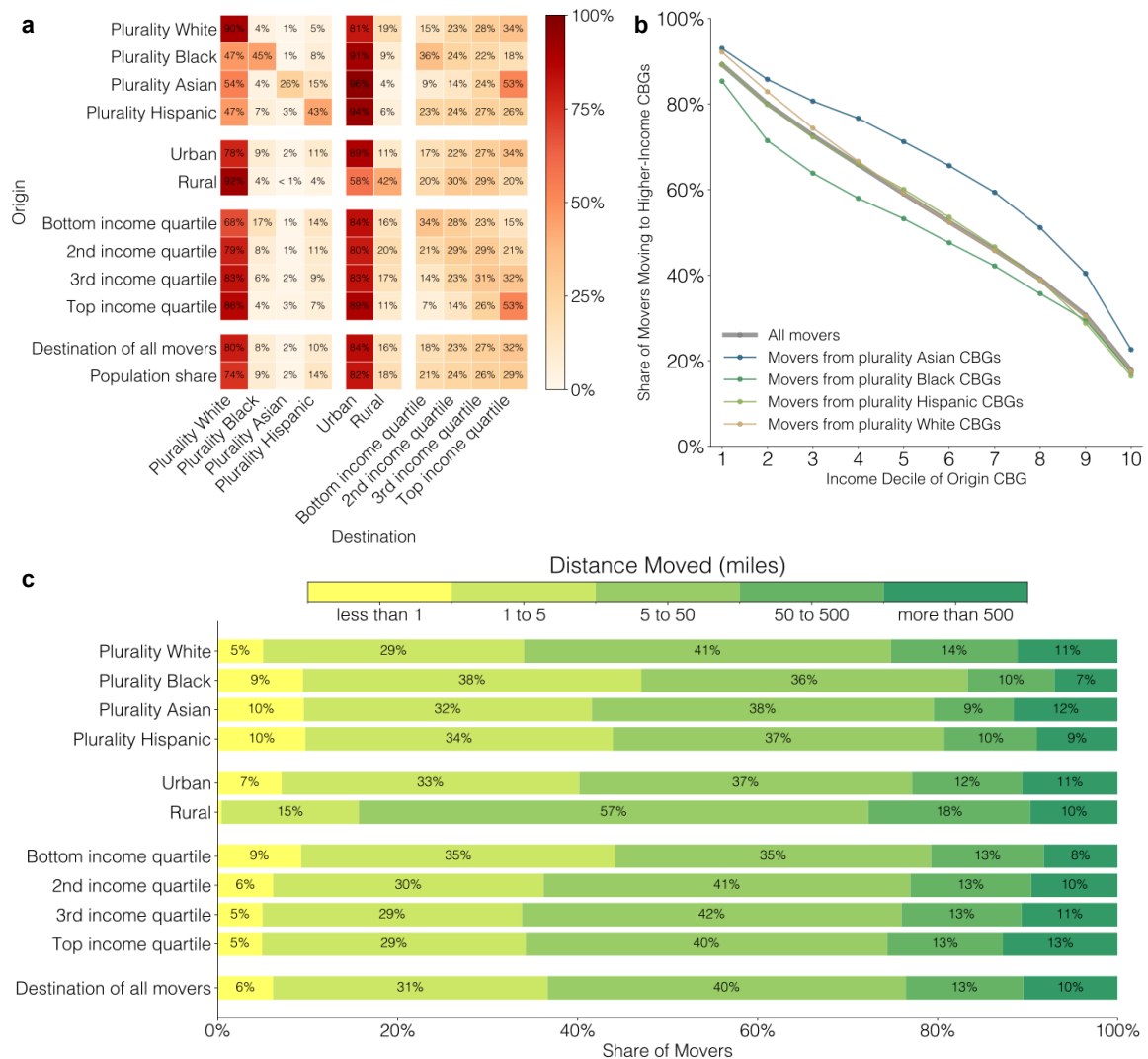


Fig. 4: National migration statistics. MIGRATE can be used to reveal fine-grained patterns of mobility across the United States. **(a)** Flows between ten types of Census Block Groups (CBGs) — plurality white, Asian, Black, and Hispanic; urban versus rural; and bottom, second, third, and top income quartile. Rows correspond to the origin CBG, and columns to the destination CBG; for example, the top left entry indicates that 90% of movers from plurality white CBGs move to plurality white CBGs. The final two rows report the proportion of all movers moving to CBGs of each type, and the population share living in CBGs of each type. We report averages across all years. **(b)** Probability of moving to a higher-median-income CBG, conditional on income decile of origin CBG, and plurality race of origin CBG. **(c)** Distance moved stratified by CBG type.

Black CBGs less likely, to move to higher-income CBGs. For example, movers from fifth-income-decile, plurality Asian CBGs have a 71% chance of moving to a higher-income CBG; movers from fifth-income-decile, plurality Black CBGs have a 53% chance. Supplementary Figure 5 shows that the same racial disparities occur when controlling for CBG median income percentile, as opposed to decile; or when examining the probability of moving to a top- or bottom-income-quartile CBG, as opposed to moving to a higher-income CBG. Overall, we find robust and substantial racial disparities in income of destination CBG that persist even conditional on income of origin CBG.

Finally, Figure 4c provides statistics on the distance of moves. 37% of movers move less than 5 miles; 40% from 5-50 miles; and 23% more than 50 miles. Figure 4c also highlights demographic variation in these statistics, revealing that movers from plurality white CBGs, rural CBGs, and higher-income CBGs are likelier to move long distances (more than 50 miles). In Appendix B.4, we report additional migration distance statistics stratified by geographic boundary (i.e., whether

movers remain within the same tract, county, or state) and show that migration distance increases over the decade we study.

Overall, these results demonstrate that fine-grained migration data illuminates important demographic variation in homophily, upward mobility, and migration distance. Future research could stratify migration flows by additional characteristics available in Census data: for example, one might study the migration patterns of immigrants by analyzing flows from areas with larger proportions of immigrants, or larger proportions of residents with a given country of birth—both of these are datasets available at the sub-county level via ACS. However, we note that such analyses require significant heterogeneity across CBGs (or other Census areas) in the demographic trait being studied; for example, it would not be possible to reliably disaggregate migration patterns by gender using this method, since gender proportions remain relatively stable across Census areas.

5 Analysis of local migration patterns

In addition to using MIGRATE to analyze national migration trends, we use it to study local migration patterns: specifically, migration in response to wildfires in California. Natural disasters, including wildfires, are known drivers of human mobility^[3,45]. There were over 3,000 fire events in California from 2010-2019, which cumulatively affected nearly 27,504 square kilometers — approximately 6.5% of the California land area. In many US states, including California, wildfire risk increased from 2010-2019^[46], and is expected to further increase due to climate change^[47]. Researchers rely on a variety of data sources, such as administrative records and building codes, to study vacancy and movement following these disasters^[48].

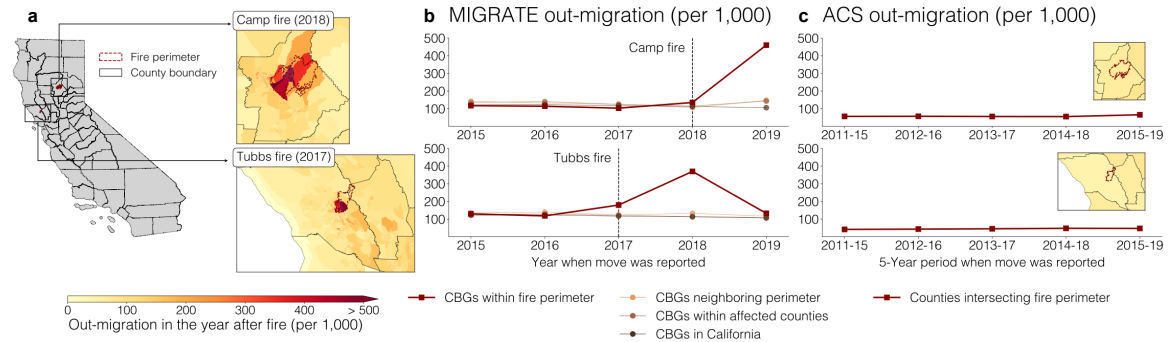


Fig. 5: Migration in response to California wildfires. (a) Out-migration following the Camp fire (2018; top) and Tubbs fire (2017; bottom). Red boundaries plot fire perimeters; black lines plot county boundaries; Census Block Groups (CBGs) are colored by domestic out-migration rate in MIGRATE. Out-migration rates exceed 50% in many CBGs within the fire perimeters. (b) Out-migration rates in different groups of CBGs over time according to MIGRATE estimates. Out-migration rates in the year after the fire are higher in CBGs within the fire perimeter (red line) than in groups of CBGs outside the fire perimeter (other lines), including those neighboring the fire perimeter, those in affected counties, or those within California. (c) Out-migration rates in the American Community Survey (ACS) 5-year county-to-county data remain relatively constant over time.

Post-wildfire migration estimates can inform disaster response and long-term planning in multiple ways. First, migration data is crucial for policymaking in the aftermath of a wildfire. It helps guide the allocation of housing, public health, and other resources to support displaced residents while minimizing strain on housing markets in receiving areas^[45,49–51]. Data on out-migration rates from affected areas can also inform decisions about whether and how to rebuild in fire-prone regions^[52,53]. Second, high-resolution migration data is important for future wildfire planning. As populations relocate in response to shifting wildfire risks, migration patterns can refine policymakers’ estimates of future risk and guide the regulation of housing and insurance markets^[54–58]. While some households may move to reduce their exposure, others may become “trapped” in high-risk areas due to financial, social, or logistical barriers^[59–61]. Identifying these communities through high-resolution migration data can help ensure that government support reaches those who need it most^[53,62].

We use high-resolution fire perimeter data from the California Department of Forestry and Fire Protection^[63]. Fire perimeters are typically much smaller than county boundaries, suggesting that

analyzing fire impacts may require the granularity of the MIGRATE estimates as opposed to the relatively coarse county-to-county flows. We analyze the two most destructive fires in California from 2010-2019 (as quantified by the number of structures lost to the fire): the Tubbs Fire in October 2017, and the Camp Fire in November 2018 (Figure 5). The Tubbs Fire occurred in Napa County and Sonoma County and destroyed at least 5,636 residential or commercial structures^[64]. The Camp Fire, about a year later, destroyed over 18,804 structures and damaged nearly 1,000 more in the Northern California county of Butte^[65]. The Camp Fire remains the most destructive wildfire in California as of early 2025; the Tubbs Fire has only been surpassed by the January 2025 Eaton and Palisades fires^[66].

MIGRATE estimates reveal dramatic levels of out-migration for CBGs within the fire perimeters (Figure 5a) in the year following the fires, often exceeding 50%⁶. In contrast, CBGs outside the fire perimeters experience much lower out-migration rates. We systematically quantify these differences in Figure 5b, which compares CBGs within the fire perimeter to three sets of less-affected CBGs outside the perimeter: (1) other CBGs neighboring the perimeter; (2) other CBGs within the affected counties; and (3) others within California as a whole. The out-migration rate in the year following the Camp Fire for CBGs within the fire perimeter is 46%, at least 3.1× that of less-affected CBG groups; the out-migration rate in the year following the Tubbs Fire for CBGs within the perimeter is 37%, at least 2.8× that of less-affected CBG groups. Our estimates of out-migration following the Camp Fire are similar to those in prior work^[45].

In contrast, publicly available county-level migration data obscure these dramatic out-migrations; Figure 5c shows that rates of out-migration in affected counties remain essentially flat. This happens because the county-level data is both too spatially and too temporally coarse: the county boundaries include many CBGs unaffected by the fire, and the estimates are aggregated over 5 years. Further, many people displaced by the Camp and Tubbs Fires moved to other CBGs within the affected counties (and thus would not be counted as movers in the county-level data): 77% of movers from CBGs within the Tubbs fire perimeter and 54% of movers from CBGs within the Butte Fire perimeter remained within the affected counties.

ACS 5-year CBG population estimates similarly obscure the dramatic levels of out-migration due to their lack of temporal granularity. In the year following the fires, MIGRATE estimates reveal population declines 260% larger in magnitude for the Tubbs fire and 40% larger in magnitude for the Camp fire than those visible at the 5-year ACS level. (For this analysis, we compare to the relative change in the ACS 5-year dataset released the year following the fire from the ACS 5-year dataset the year before: for example, for the 2018 Camp Fire, we compare the 2015-2019 ACS estimates to the 2014-2018 ACS estimates.) The ACS 5-year population estimates, unlike MIGRATE estimates, also provide no insight into the destinations of out-movers.

In Appendix C, we provide two additional analyses of local migration patterns that are impossible using county-level data: we analyze socioeconomic variation in New York City out-mover destinations, and migration patterns for residents who live in public housing provided by the New York City Housing Authority as part of the city’s affordable housing policy. Collectively, these analyses showcase how MIGRATE estimates reveal important, policy-relevant local migration patterns that traditional data sources conceal.

6 Discussion

We produce MIGRATE, a dataset of spatially and temporally fine-grained migration matrices capturing annual flows between pairs of CBGs from 2010-2019. Our estimates are approximately 4,600 times more spatially granular than publicly available county-to-county 5-year migration data, and 18 million times more spatially granular than state-to-state 1-year migration data. MIGRATE estimates correlate highly with external Census ground-truth datasets and reduce error and demographic bias relative to raw proprietary data. Our estimates are available for non-profit research use at migrate.tech.cornell.edu. We discuss the measures taken to protect the privacy of all individuals in the dataset in the Supplementary Information.

We use MIGRATE to analyze both local and national patterns of migration. We show that MIGRATE can reveal important local migration patterns, including dramatic increases in out-migration in response to California wildfires, that are invisible in county-level data. Nationally, we

⁶The fact that the out-migration rate is not 100% is likely due to a number of factors, including the often-preferred option of rebuilding and returning^[56,57], and is consistent with past studies finding a much more significant uptick in short-term vacancy than in long-term vacancy^[48].

analyze demographic and temporal variation in migration patterns. We find that people tend to move to CBGs of the same type across dimensions of race, income, and rural/urban status — for example, movers from plurality Black, Asian, and Hispanic CBGs are $15.5\times$, $14.6\times$, and $4.3\times$ likelier to move to CBGs with the same plurality race group, consistent with prior work documenting the persistence of racial segregation^[67–69]. We document demographic and temporal variation in moving distance: movers from plurality white, rural, and higher-income CBGs are likelier to travel long distances, and moving distance increases over the decade we study, consistent with prior work^[25].

An important finding from our national analysis is racial and temporal variation in upward mobility. Movers are likelier to move to top-income-quartile CBGs than bottom-income-quartile CBGs, a trend that becomes more pronounced over the decade we study. We find large racial disparities in the likelihood of moving to higher-income CBGs, or top-income-quartile CBGs, even when controlling for income of origin CBG: movers from plurality Asian CBGs are likelier to move to a higher-income CBG, and movers from plurality Black CBGs are less likely. These findings are consistent with prior work documenting racial disparities in neighborhood attainment^[70–73] and generalize these findings to larger and more recent samples and additional racial groups. Overall, we document demographic and temporal variation in national migration trends using a recent, large-scale, and highly granular dataset.

While we validate MIGRATE estimates comprehensively against external data sources, practitioners making use of the data should be mindful of two limitations. First, while we use multiple ground-truth Census data sources to reduce the biases we document in the raw Infutor data, uncorrected biases likely remain. For example, while we correct biases in CBG populations, we cannot correct sub-CBG-level population biases, or biases in CBG-CBG flows; practitioners should thus not assume data at this level contain no residual biases. Data at very fine-grained levels will also be noisier than data at more aggregated levels; while we provide practitioners with fine-grained data to maximize flexibility, we recommend aggregating up to less fine-grained levels if granularity is not required for analysis. Second, while we show that MIGRATE estimates are highly correlated with external Census datasets (including held-out datasets that are not used to produce our estimates), these validations have imperfections. As we further describe in the Methods Section, Census datasets themselves have biases; are not perfectly consistent with each other; and can possess significant margins of error, particularly at fine spatial scales. To mitigate these concerns, we conduct our harmonization process using datasets with relatively low margins of error and also prioritize fitting to Census datasets that are more precisely estimated (both detailed in the Methods Section). Another challenge in validation is the lack of a ground-truth CBG-CBG migration matrix against which to validate; publicly available Census datasets do not afford this level of granularity, and non-Census data sources (e.g., voter files) have significant biases and measure substantively different populations than the one we seek to model^[41,74,75]. Overall, MIGRATE should be viewed as a migration data source that like all data possesses limitations but that nonetheless represents a significant improvement on widely used publicly available data sources (due to its granularity) or proprietary data sources (due to reductions in error and bias).

We hope these improvements will enable a wide range of further migration-related analyses. As our analyses illustrate, MIGRATE reveals patterns which cannot be observed in publicly available, county-level migration data. We release MIGRATE as a resource to facilitate more precise study of many migration-related phenomena across the social, health, urban, and environmental sciences.

Methods

M.1 Processing Infutor Data

Infutor provides data in tabular form. Each row in the data provides data for one individual, which includes a list of known addresses, along with the date when the individual is first observed at the address (which we refer to as the effective date below), and the first and last date that the individual is observed in the data (which we refer to as the listed start date and the listed end date, respectively). Dates are listed as month and year. For example, the data for one individual might consist of two addresses: “1 Main Street, Everytown, USA, 10000 (January 2010); 2 Cornelia Street, New York, New York, USA (December 2017)” followed by an initial date of January 2008 and an end date of December 2017. We describe the steps taken to (1) identify and clean Infutor data records within the scope of MIGRATE, (2) process the Infutor data into matrices documenting yearly flows between address pairs, and (3) map these address-level matrices to the CBG-level matrices $E^{(t)}$ mentioned in the main text. Table 2 summarizes the raw and processed data.

Cleaning address histories

We first create a sequence of monthly addresses for each individual in Infutor: i.e., the address at which they are living each month. This requires us to resolve any inconsistencies in the dates provided by Infutor and model uncertainty in address histories.

We define the interval of activity during which each individual is active (observed) in the Infutor data. For each individual, we define their reconciled start date as the minimum of their first effective date, and their listed start date. We similarly define their reconciled end date as the maximum of their last effective date, and their listed end date. (For example, if the effective date list for an individual was [January 2013, January 2016], their listed start date was January 2014, and their listed end date was January 2017, their reconciled start date would be January 2013, and their reconciled end date would be January 2017.) Finally, we define their interval of activity as [reconciled start date – 1 year, reconciled end date + 1 year]. We use 1-year padding to reflect the annual granularity of the final dataset we produce and avoid discarding data in each yearly estimation process. This padding is also consistent with our treatment of deaths and emigrants, who will be recorded as non-movers in MIGRATE (and thus keep residence in the address they held during their last year alive in the United States).

Having defined each individual’s interval of activity, we define the address at which the individual is located for each month in that interval. This requires us to resolve inconsistencies in the address dates provided by Infutor, which we do as follows. We discard any addresses lacking an effective date, unless they are the only address for the individual—in such cases, we consider the reconciled start date also to be the effective date for that address. We discard any postal box addresses if there is a non-postal box address for an individual with an effective date within a year, since we assume that non-postal-box addresses are more reliable indicators of where someone lives. We then forward fill the remaining addresses so that each address spans the period between its own effective date and the effective date of the next address. If the reconciled start date and reconciled end date for the individual differ from all the address effective dates, we fill these gaps with the first and last available addresses chronologically. If the individual has multiple addresses with the same effective date, we uniformly split the individual between the addresses by saying there was an equal probability of residence in any of them. At the end of this process, each individual is associated with a monthly probability distribution over addresses for each month in their interval of activity.

Processing address histories into annual address-address migration matrices

We then aggregate the monthly address histories for each individual to the annual level in a way which is consistent with the ACS interview process. We will ultimately reconcile the Infutor data with ACS geographic mobility data and thus want these datasets to be consistently processed. Our goal is to simulate the sampling process of ACS, in which any individual can be asked, throughout the year, where they lived one year ago (the specific wording of the ACS interview question is, “Where did this person live 1 year ago?”). To do so, we loop over the twelve months of the year and compute how the individual would answer this survey question if they were asked in each month, yielding flows between a pairs of addresses (where the individual currently resides, and where they resided a year prior).

We allow monthly flows to be probabilistic. For each pair of months in which the individual was certainly seen at single addresses, they would notify the ACS of that move (or stay) with probability one. However, if in one of the months there was uncertainty due to conflicting effective dates, the corresponding flow will also be uncertain; the individual might notify ACS they moved from *any* of the addresses they resided in the previous year during the month, or to *any* of the addresses they reside in the current year. We multiply probabilities of residence in each different address to obtain the probability of a flow; if the monthly address distribution remains constant in both years we assume permanence (i.e. the individual did not move) and report that individual possibly stayed in each listed address with its own residence probability. Accounting for this uncertainty yields a list with 3-tuples of addresses and a probability (ADDR1, ADDR2, $p_{1 \rightarrow 2}$) per month; weighting these tuples per month (according to the number of days in the month) yields an yearly distribution.

We then aggregate these yearly distributions over the entire Infutor data, we create a list of expected ACS responses for the full population. That is, if multiple people reported a flow between ADDR1 and ADDR2, we add all their individual probabilities and report a single combined flow between ADDR1 and ADDR2. This represents the expected number of individuals with that flow reported to ACS. Finally, we create an yearly set of matrices $A^{(t)}$ with dimension $N_{\text{ADDRESSES}} \times N_{\text{ADDRESSES}}$ (i.e. a square matrix on the number of unique Infutor addresses) where each entry $A_{ij}^{(t)}$ corresponds to the expected number of individuals moving between addresses i and j from year $t-1$ to year t . These matrices will be further aggregated based on the location of each address.

Processing address-address migration matrices into CBG-CBG migration matrices

We transform the address-level migration matrices $A^{(t)}$ into CBG-level matrices $E^{(t)}$ by mapping each address either to a precise CBG where possible, or to a distribution over CBGs when only a ZIP code is available. We use the 2010 Census block group boundaries for all addresses to maintain geographic consistency. Figure 6 details this process.

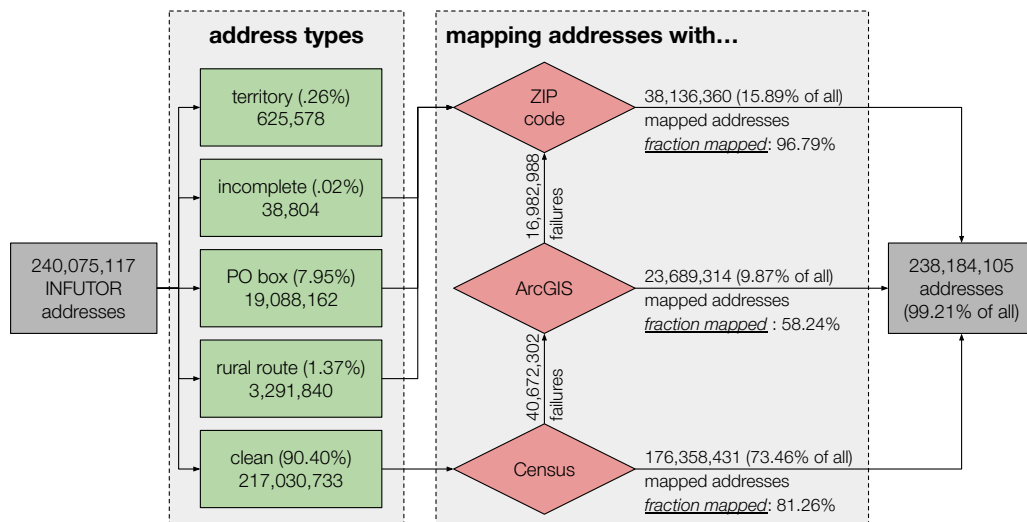


Fig. 6: Geocoding overview. Flowchart detailing the process of mapping addresses to Census Block Groups (CBGs). We start with all Infutor addresses and classify them into five address types. We remove addresses which lie within US territories but not US states (around .26% of the addresses). Incomplete addresses—those that do not have a precise street address line—as well as PO boxes and rural routes are mapped probabilistically to CBGs according to their ZIP code. The vast majority (90.4%) of addresses are clean, complete street addresses which are sent to the Census geocoder, which is able to map 81.26% of these addresses to a Census block group. If the Census geocoder fails to provide a match, we reattempt matching using ESRI’s ArcGIS geocoder; this achieves a lower match rate of 58.24%, in part because the sample it is applied to is more difficult to parse. In total, we are able to map 99.21% of all addresses in the original Infutor data: 83.33% to a precise latitude and longitude, and 15.89% to a ZIP code.

Our address mapping pipeline is divided in two parts: mapping addresses via geocoding, and mapping addresses with a ZIP code-to-CBG crosswalk. We initially attempt to use one of two state-of-the-art geocoders to map addresses to latitudes and longitudes: the publicly-available Census Bureau geocoder [43] and ESRI’s ArcGIS geocoder [42]. We first attempt to geocode an address via the Census geocoder; if this algorithm does not find a match, we submit the address to ArcGIS. If neither algorithm finds a match, we map the address to Census Tracts intersecting its ZIP code, weighting probabilities based on the share of residential ZIP code addresses represented by the population of each Census Tract. Addresses representing rural routes and postal boxes are directly mapped via ZIP code, as well as incomplete addresses. We use the HUD ZIP-to-tract crosswalk, with the date closest available to the last seen date of an address to account for the fact that ZIP code definitions may vary and are not nested within Census geographies [76]. We then distribute the probability to each Census block group within the tracts, again weighting by their relative population shares. Success rates for each of these steps are high and detailed in Figure 6.

We use the results of this mapping process to create an auxiliary matrix \mathcal{G} of dimensions $N_{\text{ADDRESSES}} \times N_{\text{CBGS}}$. Each row of \mathcal{G} defines a probability distribution over Census block groups: an address i belongs to CBG j with probability \mathcal{G}_{ij} . If the address has been precisely mapped (i.e., geocoded via the Census or ArcGIS geocoders), the corresponding row of \mathcal{G} has a single entry equal to 1, with other entries 0. We use the matrix \mathcal{G} to compute the CBG-to-CBG matrix $E^{(t)}$ via the following equation:

$$E^{(t)} = \mathcal{G}^T \cdot \left[A^{(t)} - \text{diag} \left(A^{(t)} \right) \right] \cdot \mathcal{G} + \text{diag} \left[\mathcal{G}^T \cdot \text{diag} \left(A^{(t)} \right) \right] \quad (1)$$

where the $\text{diag}(\cdot)$ operator either converts a vector into a diagonal matrix or extracts the diagonal of a matrix as a vector. The first term in this equation maps movers to the appropriate entries of the migration matrix: for example, a precisely mapped move from CBG i to CBG j will increment $E_{ij}^{(t)}$ by 1, and a move from ZIP code a to ZIP code b will distribute mass (summing to 1) evenly across the sub-block whose rows lie within ZIP code a and columns lie within ZIP code b . The second term in this equation maps stayers to the appropriate diagonal entries of the migration matrix: for example, a precisely mapped stayer in CBG i will increment $E_{ii}^{(t)}$ by 1, and someone who stays within ZIP code a will distribute mass (summing to 1) evenly across the diagonal entries corresponding to CBGs within that ZIP code.

Summarizing the Processed Infutor Data

Table 2 reports a yearly breakdown of relevant Infutor data statistics throughout this pipeline. The number of individuals with active records in the data represents the number of individuals with an interval of activity containing each year at the start of the data processing; the number of CBG moves corresponds to the sum of off-diagonal entries of each matrix $E^{(t+1)}$ and measures the “effective size” of each year’s data: how many movers we actually account for at the beginning of the estimation procedure.

Year	(1) Active records	(2) US Population	(3) Processed CBG Moves
2010	269,228,776	309,327,143	15,180,982
2011	260,064,921	311,583,481	11,793,806
2012	259,451,204	313,877,662	12,544,199
2013	252,933,953	316,059,947	13,829,056
2014	256,453,630	318,386,329	13,071,070
2015	241,295,957	320,738,994	14,022,249
2016	242,298,262	323,071,755	13,605,804
2017	193,479,001	325,122,128	12,684,184
2018	177,629,604	326,838,199	13,505,890

Table 2: Yearly Breakdown of Data Summaries. Population and addresses accounted by the Infutor and Census datasets during the analysis period (2010-2019). **(1)** Individuals have active records in a given year if the year falls within their interval of activity in the dataset. Comparison of these values to **(2)** the Census population shows that Infutor under-counts the population at every given year. **(3)** The number of moves between Census Block Groups (CBGs) parsed in our dataset. Note that an individual with two addresses will have at most one move, some addresses do not constitute residences, some individuals may have a single address in the year thus not move, etc.

The number of active records drops in recent years because individuals are only marked as “active” when they have a recorded move; many people simply haven’t had a recent move, so they no longer appear as active even though they remain in the population. This means that Infutor is more likely to underrepresent non-movers in recent years. We employ several measures to mitigate this effect: we pad each individual’s reconciled end date by one year when constructing their active interval, and also rescale Infutor data to match rates of non-movers in Census data.

We also verify that the decrease in Infutor active records in recent years, which is simply an expected consequence of how active records are defined, does not reflect a broader and more worrisome decrease in Infutor data quality over time. To do this, we examine variation over time in the quality metrics discussed in the validations section — the RMSE and correlation between Infutor and Census data for population counts, mover counts, and in-migration rates. Results are shown in Table 3. While some quality metrics improve slightly over time, and others worsen slightly, overall we do not find consistent evidence that processed Infutor data quality decreases over time.

Quantity	Dataset	2011	2012	2013	2014	2015	2016	2017	2018	2019
CBG Population	Infutor	-	-	-	507	519	531	556	581	-
	MIGRATE	-	-	-	80	91	91	91	88	-
State-to-State Movers	Infutor	3,031	3,684	3,549	3,372	3,607	3,315	2,801	2,518	2,431
	MIGRATE	365	403	400	399	434	410	343	361	383
State In-Migration Rate (per 1,000)	Infutor	12.4	14.9	14.4	13.4	14.1	12.4	9.77	6.78	5.56
	MIGRATE	1.68	1.73	1.92	1.48	1.29	1.18	1.07	1.03	1.12

(a) Root mean squared error (RMSE) for Infutor and MIGRATE, compared to Census data.

Quantity	Dataset	2011	2012	2013	2014	2015	2016	2017	2018	2019
CBG Population	Infutor	-	-	-	0.824	0.826	0.827	0.822	0.818	-
	MIGRATE	-	-	-	0.996	0.995	0.995	0.996	0.996	-
State-to-State Movers	Infutor	0.950	0.956	0.953	0.951	0.954	0.950	0.948	0.936	0.919
	MIGRATE	0.998	0.997	0.997	0.998	0.997	0.998	0.998	0.998	0.998
State In-Migration Rate	Infutor	0.895	0.916	0.911	0.884	0.885	0.896	0.871	0.863	0.809
	MIGRATE	0.980	0.981	0.976	0.987	0.991	0.992	0.993	0.994	0.992

(b) Pearson correlation for Infutor and MIGRATE, compared to Census data.

Table 3: Validation of Infutor and MIGRATE estimates over time. Year corresponds to year of the Census data release. 5-Year estimates of Census Block Group Populations are only validated against matrices from 2014 to 2019, which span the full 5-year period. Metrics for in-migration rates are weighted by population area. More details on computation of these metrics can be found on our validations section.

Our harmonization process further improves the temporal stability of quality metrics, as can be seen in the MIGRATE rows of Table 3; the correlations between MIGRATE and Census data remain stable and high for all years.

M.2 Processing Census Data

The U.S. Census Bureau runs multiple programs with the aim of counting and estimating demographic and socioeconomic population data. Each of these programs may release data at different spatiotemporal granularity and, even if geographies or timespans agree, the data might lack internal consistency. We use a series of steps to clean, select, and process Census datasets. We describe our procedures for reconciling Census geographies, selecting which Census datasets to use as constraints, and how we process the Census data to deal consistently with births, deaths, emigration, and immigration.

Reconciling Census geographies

The United States is hierarchically divided into states, counties, Census tracts, Census block groups, and Census blocks, with each level subdividing its parent geography. Geographic boundaries are not necessarily consistent over time, and ensuring that population counts reflect the same geographic area across multiple years is essential when working with longitudinal data. For example, to produce multi-year estimates, the American Community Survey maps every reported address to the corresponding

geography in the *current* year^[77]. We use the 2010 Census boundaries for all addresses to maintain geographic consistency.

While the vast majority of geographies remain intact in the inter-decennial period (between Censuses, 2010-2020), there are some geography changes we must address. When geographies merge or split throughout the decade, we resolve the change by keeping only the coarser geographic boundary — i.e., the combined area which is the union of all finer-grained areas. With this approach, we can aggregate population statistics from the fine-grained areas into the coarse areas. There was one such county change in 2010-2019 affecting Bedford County in Virginia^[78] and a few Census tract or Census block group changes documented yearly in the Census Bureau website (e.g.^[79] for 2010 to 2011). When we aggregate ACS estimates that contain margins of error, we also aggregate margins of error in the L2 norm—as proposed by the ACS^[80]. For our purposes, area renames are irrelevant. After these adjustments, MIGRATE considers a universe of 217,740 Census block groups grouped into 3,142 counties.

Selecting Census datasets

We rely primarily on three Census datasets: the ACS 5-year CBG populations; ACS 1-year state-to-state flows (from which we use raw flows as well as counts of non-movers and movers); and PEP 1-year county populations. PEP makes use of administrative records on births, deaths, and net migration to directly estimate county-level populations; the numbers reported contain the population estimate for July 1st of every year. ACS estimates, on the other hand, are a product of year-round surveying aggregated at the correspondent time scale, then released with associated margins of errors that define 90% confidence intervals^[80]. Our dataset selection and methodology accounts for these different precision levels across the board.

We would like to avoid matching to datasets that were too noisily estimated. To decide which ACS datasets to use in our harmonization process, we examine their level of sampling error. We quantify the sampling error by the coefficient of variation (CV): the ratio of the standard deviation to the estimate value. Table 4 reports the mean coefficient of variation in ACS estimates. In general, the number of non-movers has very low CVs (mean below 2% for counties and below 1% for states); population estimates have considerably lower CVs than flow estimates; state-to-state flows have relatively high CVs (mean around 45% every year), and county-to-county flows have extremely high CVs (mean almost 90%). We opt not to match to county-county flows due to the imprecision of raw flow estimates, although we do use them as a validation. In-migration rates have much tighter CVs than the corresponding flows (mean around 15% and 5% for counties and states, respectively), and we also use those as validations.

	2010	2011	2012	2013	2014	2015	2016	2017	2018	2019
CBG Populations	15.76	15.67	15.42	15.33	15.17	14.94	14.95	15.08	15.21	15.59
Tract Populations	6.41	6.24	6.03	5.95	5.79	5.60	5.50	5.54	5.56	5.66
County Flows	-	91.03	89.97	89.47	89.41	88.06	87.33	87.30	87.01	87.01
County Non-Movers	-	1.78	1.72	1.69	1.68	1.65	1.64	1.65	1.63	1.65
County In-Migration Rate	-	16.37	15.79	15.55	15.48	15.03	14.96	15.25	15.34	15.60
State Flows	-	47.61	45.47	45.14	44.23	45.33	45.76	46.31	45.62	47.31
State Non-Movers	-	0.41	0.39	0.39	0.38	0.40	0.40	0.38	0.37	0.39
State In-Migration Rate	-	4.95	4.68	4.79	4.65	4.70	4.76	4.72	4.85	5.02

Table 4: Uncertainty in Census datasets. Average coefficient of variation (CV) of the non-zero estimates in each American Community Survey (ACS) dataset (in %). CVs were computed as the ratio of the standard error (obtained by dividing the margin of error by 1.645) by the estimate^[80]. We did not use flows released in 2010 (as they would report moves from 2009).

We perform a synthetic simulation study to verify that the datasets we do match to — state-to-state flows, and CBG population estimates — have sufficiently low sampling error to be reliably used. In particular, we resample each dataset using its reported margins of error, and compute correlations between the resampled data and the original data. To also assess mobility rates, we summarize state-to-state flows via the net migration rate. CBG populations and net state migration rates remain highly correlated with themselves after resampling (average Pearson correlation of $\rho = 0.976$ and $\rho = 0.766$, respectively).

Based on these analyses, we harmonize the entries of each yearly matrix $E^{(t)}$ with the following data: (1) CBG populations (both from 2010 Census and 5-year ACS); (2) ACS 1-year counts of

movers and non-movers by state; (3) ACS 1-year state-to-state flows; and (4) PEP 1-year county populations. Population count data at the sub-county level was obtained via IPUMS National Historical Geographic Information System, along with socioeconomic and demographic data used for our bias analyses^[81]; population flows and movers data was obtained directly via ACS^[82]; population count data at county level was obtained via the Population Estimates Program^[83].

Accounting for natural population increase and international migration

Using Census datasets to constrain MIGRATE estimates requires ensuring that the Census datasets reflect the same population accounted for in the Infutor matrix $E^{(t)}$. Each entry $E_{ij}^{(t)}$ represents the expected number of people alive with a residence in area i at year $t-1$ and with a residence in area j at year t , and diagonal entries $E_{ii}^{(t)}$ also include individuals who resided in area i at year $t-1$ but died or emigrated. We process the Census datasets so they reflect the same population, by accounting for changes in the populations at year t due to births, deaths, and international migration. Specifically, when using Census populations from year t to scale entries of $E^{(t)}$, we want to remove from each Census area population the natural increase in population (i.e., births minus deaths) and the net international migration (i.e., immigrants minus emigrants); when using Census flows from year $t-1$ to year t , we want to add counts of deaths and emigrants back into the diagonal as non-movers. We adjust the Census constraints individually for every matrix $E^{(t)}$.

To do this adjustment, we make use of the PEP components of population change and ACS international immigration estimates. PEP releases estimates for the number of births, deaths, net international migration, and net domestic migration yearly at both a county and a state level^[83]. To build yearly population estimates, PEP directly adds to the previous year’s estimates the natural increase, net international migration, and net domestic migration⁷. Whereas PEP estimates only report the net international migration, the ACS 1-year state-to-state flows also estimate the yearly number of immigrants per state (average CV around 12% across all years), which allows us to estimate the number of emigrants per state.

M.3 Harmonizing Infutor and Census Data

Having processed the Infutor and Census data, the final step in producing MIGRATE is to harmonize both data sources. Our harmonization process consists of scaling selected entries of the $E^{(t)}$ to match non-zero entries of Census datasets. We do not scale any entries to zero because the Census zeroes are noisily estimated, and subsequent multiplicative re-scalings cannot correct erroneous zero scalings. We detail below, in order, the scalings we perform.

Harmonizing with CBG population data

First, we harmonize $E^{(t)}$ with CBG populations from the 5-year ACS estimates and the 2010 Census. We scale each row of each matrix $E^{(t)}$ such that the row sums — i.e., the CBG populations — are consistent with the constraints implied by the ACS 5-year CBG populations and the 2010 Census. For example, when we take the average sum of each row across the five matrices $\{E^{(2011)}, E^{(2012)}, E^{(2013)}, E^{(2014)}, E^{(2015)}\}$, this should be equivalent to the population for the corresponding CBG in the 2011-2015 ACS. We also impose a boundary constraint to match the 2010 population to that reported by the Decennial Census. Imposing these constraints corresponds to solving the non-negative least squares optimization problem

$$\begin{aligned} \text{minimize} \quad & \|A \cdot \vec{x} - \vec{b}\| \\ \text{s.t.} \quad & \vec{x} \geq 0 \end{aligned} \tag{2}$$

⁷PEP produces estimates that are geographically consistent: county-level estimates must aggregate precisely to state-level estimates, which must aggregate to nation-level estimates^[83]. To achieve such precision, they also estimate small residuals at the county and state levels. We ignore these values.

where

$$A = \begin{pmatrix} 0 & 1 & 0 & 0 & 0 & 0 & 0 & 0 & 0 & 0 & 0 \\ \frac{1}{2} & \frac{1}{2} & 0 & 0 & 0 & 0 & 0 & 0 & 0 & 0 & 0 \\ \frac{1}{3} & \frac{1}{3} & \frac{1}{3} & 0 & 0 & 0 & 0 & 0 & 0 & 0 & 0 \\ \frac{1}{4} & \frac{1}{4} & \frac{1}{4} & \frac{1}{4} & 0 & 0 & 0 & 0 & 0 & 0 & 0 \\ \frac{1}{5} & \frac{1}{5} & \frac{1}{5} & \frac{1}{5} & \frac{1}{5} & 0 & 0 & 0 & 0 & 0 & 0 \\ 0 & \frac{1}{5} & \frac{1}{5} & \frac{1}{5} & \frac{1}{5} & \frac{1}{5} & 0 & 0 & 0 & 0 & 0 \\ 0 & 0 & \frac{1}{5} & \frac{1}{5} & \frac{1}{5} & \frac{1}{5} & \frac{1}{5} & 0 & 0 & 0 & 0 \\ 0 & 0 & 0 & \frac{1}{5} & \frac{1}{5} & \frac{1}{5} & \frac{1}{5} & \frac{1}{5} & 0 & 0 & 0 \\ 0 & 0 & 0 & 0 & \frac{1}{5} & \frac{1}{5} & \frac{1}{5} & \frac{1}{5} & \frac{1}{5} & 0 & 0 \\ 0 & 0 & 0 & 0 & 0 & \frac{1}{5} & \frac{1}{5} & \frac{1}{5} & \frac{1}{5} & \frac{1}{5} & 0 \\ 0 & 0 & 0 & 0 & 0 & 0 & \frac{1}{5} & \frac{1}{5} & \frac{1}{5} & \frac{1}{5} & \frac{1}{5} \end{pmatrix} \quad \vec{b} = \begin{pmatrix} \text{Census}_{2010} \\ \text{ACS}_{2006-10} \\ \text{ACS}_{2007-11} \\ \text{ACS}_{2008-12} \\ \text{ACS}_{2009-13} \\ \text{ACS}_{2010-14} \\ \text{ACS}_{2011-15} \\ \text{ACS}_{2012-16} \\ \text{ACS}_{2013-17} \\ \text{ACS}_{2014-18} \\ \text{ACS}_{2015-19} \end{pmatrix}$$

for each row (i.e. each CBG). The vector \vec{x} represents the estimated population for the CBG in each year from 2009 to 2019, and we impose the constraint that $\vec{x} \geq 0$ to ensure populations are non-negative. We use these estimated CBG populations to harmonize our flow matrices, by scaling each row to match the estimated CBG population in the relevant year.

Harmonizing with yearly data on state movers and non-movers

Next, we harmonize $E^{(t)}$ with the counts of movers and non-movers by state from 1-year ACS data. To do this, we aggregate the off-diagonal entries of columns corresponding to each state and scale them to match the count of movers by state. We also aggregate the diagonal entries of columns corresponding to each state and scale them to match the count of non-movers by state. These scalings (which treat the population remaining within each CBG as equivalent to the population of non-movers) assume that very few people move to another location within the same CBG, an assumption substantiated by previous research: the median distance people moved in the US was about 10 to 15 miles in the 2010-19 period, which is far more than the average 2010 CBG radius (1.7 miles) and close to the 98th percentile of CBG radii^[84].

Mathematically, let $S_k^{(t)}$ be population of state k in year t and $R_k^{(t)}$ the population of state k in year t which did not move in the previous year. Then we multiply every diagonal entry $E_{xx}^{(t)}$ where CBG x lies in state r by

$$\frac{R_r^{(t)}}{\sum_i E_{ii}^{(t)} \cdot \mathbf{1}\{\text{CBG } i \in \text{state } r\}} \quad (3)$$

and then multiply every off-diagonal entry $E_{xy}^{(t)}$ ($x \neq y$) where CBG x lies in state r and CBG y lies in state s by

$$\frac{S_s^{(t)} - R_s^{(t)}}{\sum_{i,j : i \neq j} E_{ij}^{(t)} \cdot \mathbf{1}\{\text{CBG } j \in \text{state } s\}} \quad (4)$$

That is, we scale the off-diagonal entries so that the columns corresponding to each state (capturing the movers into that state) match the Census population who live in the state and did not live there the year prior ($S_s^{(t)} - R_s^{(t)}$).

Harmonizing with yearly state-to-state flow data

We then harmonize $E^{(t)}$ with all state-to-state flows from 1-year ACS data. To do this, we aggregate the entries of the matrix $E^{(t)}$ according to the origin-destination state pair they belong to. For example, all flows from CBGs within Delaware to CBGs within Nevada are aggregated and scaled so that they sum to the total flow from Delaware to Nevada in ACS data. We do not scale to match zero flows.

Mathematically, let $F_{rs}^{(t)}$ be the number of movers between states r and s from year $t-1$ to year t . Then we multiply every entry $E_{xy}^{(t)}$ where CBG x lies in state r and CBG y lies in state s by

$$\frac{F_{rs}^{(t)}}{\sum_{i,j} E_{ij}^{(t)} \cdot \mathbf{1}\{\text{CBG } i \in \text{state } r\} \cdot \mathbf{1}\{\text{CBG } j \in \text{state } s\}} \quad (5)$$

whenever $F_{rs}^{(t)} \neq 0$. We scale both people who move between states ($r \neq s$) and who remain within the same state ($r = s$).

Harmonizing with yearly county population data

Finally, we harmonize $E^{(t)}$ with county populations from 1-year PEP data. We choose to match $E^{(t)}$ to PEP populations last due to their superior reliability. In addition, PEP estimates are used internally by the Census Bureau as controls for many other datasets^[85], and ensuring MIGRATE estimates agree with PEP can lead to better downstream agreement in other datasets.

To match to PEP county populations, we apply a classical IPF-based algorithm, alternating between two steps until convergence: (1) we aggregate the entries of $E^{(t)}$ by columns corresponding to each county and scale them to match the PEP county population at year t and (2) we aggregate the entries of $E^{(t)}$ by rows corresponding to each county and scale them to match the PEP county population at year $t - 1$.

More formally, let $P_c^{(t)}$ be the population of a given county c at a given year t . We start with the matrix $M^0 := E^{(t)}$. We then perform the following updates for iterations $n = 1, 2, \dots, N$. For odd n , we scale the blocks of columns of the matrix to match the county populations in year t . Specifically, for each CBG y lying within county q , we multiply entries M_{xy}^{n-1} by the scaling factor

$$\frac{P_q^{(t)}}{\sum_{i,j} M_{ij}^{n-1} \cdot \mathbf{1}\{\text{CBG } j \in \text{county } q\}} \tag{6}$$

For even n , we scale blocks of rows of the matrix to match the county populations in year $t - 1$. Specifically, for each CBG x lying within county p , we multiply entries M_{xy}^{n-1} by the scaling factor

$$\frac{P_p^{(t-1)}}{\sum_{i,j} M_{ij}^{n-1} \cdot \mathbf{1}\{\text{CBG } i \in \text{county } p\}} \tag{7}$$

Our algorithm runs for 6,000 iterations, which we verify is sufficient for convergence. Specifically, we track the L1 distance between the resulting matrices in two subsequent iterations.

Appendix A Additional details on validations

Here we provide additional details on MIGRATE validations. We include additional details on our held-out data validations; a semi-synthetic data validation where we verify our method reconstructs a known ground-truth matrix; details on related work documenting biases of Infutor, which is the subject of our Figure 3; and additional socioeconomic and demographic dimensions on which we assessed biases, including undocumented immigrants.

A.1 Validating the estimation procedure using held-out data

		MIGRATE	CBG Held-Out	State Held-Out
Population counts	State	1.000	1.000	1.000
	County	1.000	1.000	1.000
	Tract	0.997	0.888	0.998
	CBG	0.996	0.856	0.997
Population flows	State	1.000	1.000	1.000
	County	1.000	1.000	1.000
Population flows (area movers only)	State	0.998	0.998	0.895
	County	0.957	0.956	0.949
Population flows (area stayers only)	State	1.000	1.000	1.000
	County	1.000	1.000	1.000
In-migration	State	0.998	0.998	0.885
	County	0.984	0.983	0.963
In-migration rate	State	0.987	0.987	0.663
	County	0.715	0.705	0.629

(a) Pearson correlation between Census data and our estimates with CBG and state data held out. Pearson correlations with MIGRATE, which is estimated using all data sources, are presented for comparison. As noted in the main text, perfect correlations between MIGRATE and all flows or stayers are partially driven by variation in area size and the predominance of non-mover counts among flows.

		MIGRATE	CBG Held-Out	State Held-Out
Population counts	State	100.00	100.00	100.00
	County	100.00	100.00	100.00
	Tract	85.88	13.46	88.13
	CBG	83.60	9.08	85.09
Population flows	State	89.46	89.40	80.87
	County	90.65	90.70	75.24
Population flows (area movers only)	State	87.46	87.06	4.08
	County	42.34	41.30	4.65
Population flows (area stayers only)	State	89.46	89.40	81.03
	County	91.01	91.08	75.59
In-migration	State	90.93	91.11	7.22
	County	68.92	68.19	6.55
In-migration rate	State	87.30	87.33	4.89
	County	51.75	50.91	0.73

(b) Reductions in RMSE. We compute RMSE between (1) our estimates and Census data and (2) Infutor data and Census data, and report the reduction in RMSE from using our estimates. Positive values indicate improvements. Values are average reductions across all years with overlapping ground-truth data releases.

Supplementary Table A1: Validation of estimates in held-out data settings. The full model validations are repeated for comparison. For in-migration rates, metrics are weighted by populations to account for disparate county and state sizes.

We verify that our estimation procedure yields highly correlated estimates with each Census data source even when it is removed from the datasets used for estimation. For example, we remove CBG-level Census populations from our estimation datasets, and verify that our resulting estimates remain highly correlated with CBG-level data. Specifically, we conduct our full battery of validations on two additional sets of migration estimates: “CBG held-out”, which is estimated without the CBG-level population data (i.e. $E^{(t)}$ was not scaled to match ACS 5-year CBG populations); and “State held-out”, which is estimated without the state-level flow data (i.e. $E^{(t)}$ was not scaled to match ACS 1-year state-to-state flows nor state mobility rates). Supplementary Table A1 reports values for the

Pearson correlation across all estimates and ground-truth as well as relative error reduction from Infutor. Values for the original MIGRATE estimates, reported in Figure 2, are reproduced for easy comparison.

The CBG held-out and State held-out estimates remain highly correlated with all Census datasets (ρ above 0.629); they also reduce RMSE relative to Infutor. Unsurprisingly, both the correlations and error reductions are smaller than those achieved by our full MIGRATE estimates, which make use of all sources of Census data. Together, these results illustrate both that (a) our estimation pipeline generalizes well to held-out data and that (b) all datasets used in the training help improve concordance with Census data, justifying their inclusion.

A.2 Validating the harmonization procedure with semi-synthetic data

We further validate our harmonization procedure using semi-synthetic data, a standard check for statistical methods when ground-truth data is lacking^[86–88]. Specifically, we assess how well our harmonization procedure can recover a known CBG-to-CBG flow matrix, given only a perturbed version of that matrix and the same set of marginal constraints available in our main analysis (e.g., CBG-level populations).

To generate realistic semi-synthetic data, we use the MIGRATE matrices as the ground-truth CBG-to-CBG flow matrices M , since these are likely more realistic than purely synthetic data generated from stylized models. These ground-truth matrices M are not used as input to our harmonization method, but only as validation. From M , we produce the perturbed CBG-to-CBG flow matrix E by adding multiplicative noise; we describe this process further below. We also compute the same marginals of M that are available in our main analysis: specifically, CBG populations; state-level counts of movers and non-movers; state-to-state flows; and county populations. We use these marginals and the perturbed matrix E as inputs to our harmonization method. We assess how well our method recovers the ground-truth matrix M using the same metrics described in the main text (reduction in RMSE relative to using E alone, and Pearson correlation).

To thoroughly test the robustness of our method, we consider two processes for generating E from M . We now describe these processes.

Harmonizing in the presence of structured multiplicative noise

Our harmonization procedure assumes that the difference between the ground-truth matrix M and the perturbed matrix E can be described by a series of multiplicative scalings with a given structure (e.g., CBG-level scalings on each row) as described in the Methods Section. We thus first test how well our harmonization procedure recovers the ground-truth matrix if the perturbation does indeed match that structure. Specifically, we draw independent Log-Normal random variables that multiply (1) each row of M (mirrors CBG population fitting), (2) each group of diagonal entries within the same state (mirrors state non-movers fitting), (3) each group of off-diagonal entries in columns within the same state (mirrors state movers fitting), (4) each group of entries within the same state-to-state pair (mirrors state flows fitting) and (5) each group of rows within the same county, and each group of columns within the same county (mirrors county population fitting). We draw the Log-Normal noise using standard deviations τ ranging from 0.05 to 0.20. We choose the upper bound on this range because it exceeds the level of variation we observe in real-world data. Specifically, across states (Figure 3a), the biases between ground-truth and Infutor populations have standard deviation 0.11; across counties, the standard deviation is 0.19, both exceeded by our upper bound of $\tau = 0.20$. (We do verify, however, that results remain robust up to much larger τ values of 1.00).

We find that our harmonization method performs very strongly in this setting. For all standard deviations of noise, our inferred matrix achieves Pearson correlations above 0.99 either on the full CBG-CBG matrix or when restricting to CBG-CBG movers. The harmonized matrix also reduces RMSE (relative to the original perturbed matrix E) by an average of 97.7% across all years and noise levels (sd 0.06%), and by 91.9% when restricting to off-diagonal entries (sd 0.67%). These RMSE reductions remain consistently strong across the range of noise scales. The small residual error is an expected result of the optimization procedure; for example, we only fit once to CBG-level marginals to avoid overfitting, so are not guaranteed to match these marginals.

Harmonizing in the presence of real-world bias and independent noise

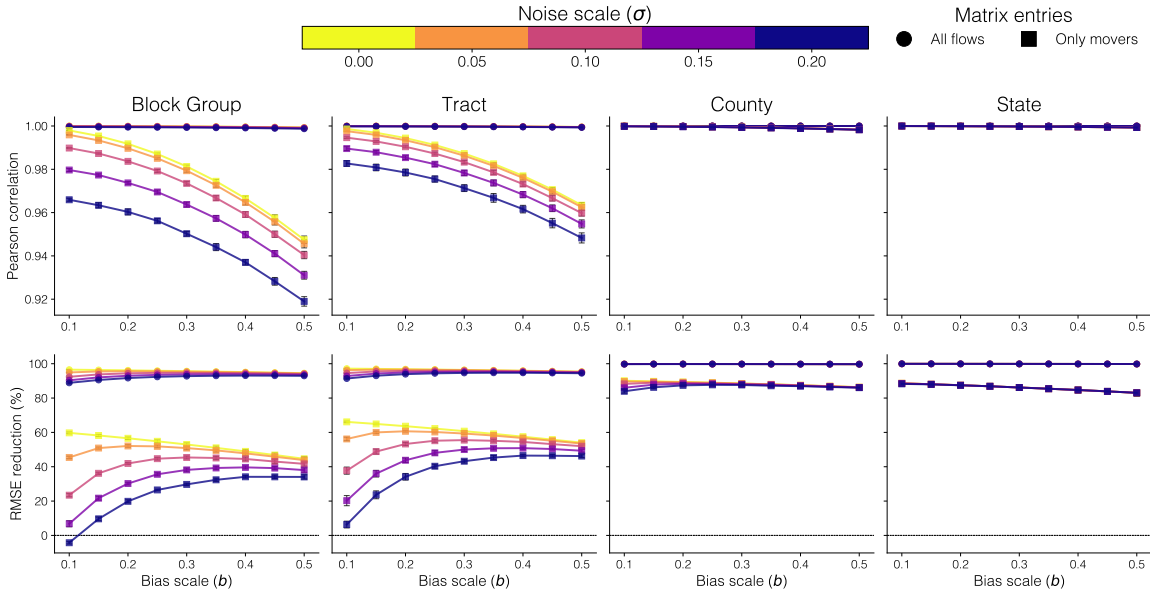
We next assess the performance of our harmonization procedure when the perturbation does not match the structure it assumes, but consists both of real-world bias and independent noise.

Specifically, we produce the perturbed matrix E from M as follows:

$$E_{ij} = M_{ij} \cdot \exp\{b \cdot (w_i + w_j) + \sigma \cdot Z_{ij}\}$$

where w_i is the z-scored share of the white population in CBG i (capturing real-world biases, as shown in Figure 3c) and Z_{ij} are i.i.d. standard normal variables. The parameters b and σ control the relative scales of the bias and the independent noise, respectively. We assess performance across a range of b and σ , choosing b to represent a realistic level of real-world bias based on our results in Figure 3c, and noise scales σ up to 0.20, as above.

We would expect high levels of independent noise to make it very challenging to recover the off-diagonal entries of the ground-truth matrix. This is because the diagonal entries of the migration matrix are much bigger than the off-diagonal entries (since most people do not move); thus, the scaling factors learned by the harmonization procedure will be dominated by the diagonal entries. This is generally reasonable: if we want to estimate bias in the movers from a CBG, the bias of the entire CBG population likely serves as a good proxy. However, this logic fails under independent noise, since noise in the diagonals provides no information about noise in the off-diagonals. Importantly, the challenge of correcting for independent noise applies not just to our harmonization procedure, but to any correction procedure, since correcting such noise would require information about the ground truth for each entry.



Supplementary Fig. A1: Experimental validations of our method. Pearson correlation and reduction in RMSE achieved by our harmonization procedure on semi-synthetic data with real-world bias and independent noise. We report average metrics across all years; error bars plot standard deviation across years (from 2010-11 to 2018-19, $n = 9$). Circles represent metrics computed on all entries of the flow matrix; squares represent metrics computed on movers only (off-diagonal elements). Columns assess metrics for flows at the CBG level, tract level, county level, and state level. We assess results when varying the level of bias (x-axis) and independent noise (line color).

Supplementary Figure A1 plots the Pearson correlation and reduction in RMSE for flows at every geographic scale. We compute metrics with respect to all flows and movers only (off-diagonal entries) for varying levels of noise and bias. Results are consistent with the analysis above. When considering all flows (as opposed to just off-diagonal entries), error is reduced almost completely and correlations are nearly perfect at all geographic scales (circular points). When restricting to off-diagonal entries specifically (square points) on the more granular geographic scales (tract and CBG levels), we find the largest error reductions when the scale of the independent noise is not too large relative to the bias, as expected. Pearson correlations decrease as bias and noise increase, but remain relatively high (above 0.91 in all cases). State and county-level metrics for movers remain robust at all noise and

bias scales because we have better marginal data with which to correct them (including state-to-state movers and county populations).

Collectively, these synthetic experiments show that our harmonization procedure performs well in recovering the ground-truth matrix as long as the structure of the perturbation lies within the family it is able to estimate; in contrast, purely independent noise is unsurprisingly harder to correct (both for our procedure and for any correction procedure). The family of perturbations our harmonization procedure can estimate is highly flexible (due to the number of scalings of varying shapes it incorporates) and indeed more flexible than classic iterative proportional fitting, which is widely used in similar demographic applications [39,40,89–91] and estimates only row and column-level scalings. The assumption that the perturbation is structured, as opposed to entirely independent for each entry, is also substantiated by our and previous findings of systematic demographic bias in Infutor data, which would not emerge under purely independent noise.

A.3 Related work documenting biases in the Infutor data

Many authors have assessed bias in the Infutor dataset, generally focusing on the data subsets or demographic characteristics most relevant to their own analyses. To our knowledge, the analysis we present in Figure 3 constitutes the first comprehensive documentation of biases in the Infutor dataset across (a) a long period of time and (b) the entire United States. We include here a non-exhaustive review of works with documentation of Infutor biases.

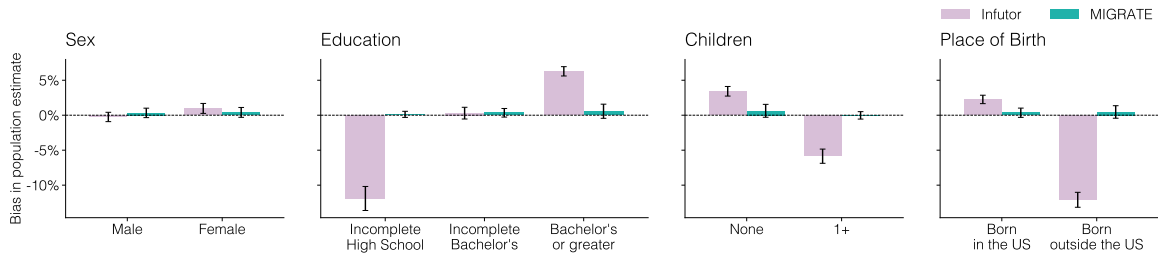
As we report in Table 2, Infutor undercounts the national US population. This is consistent with prior work; a similar finding is reported by Qian and Tan [32], Bernstein et al. [30], and Diamond et al. [27] among others. Phillips [13] additionally reports that, relative to 2010 ACS data, Infutor undercounts all state populations, but not by much, and out-of-state movers. A contrasting finding, reported by Diamond et al. [5], is that Infutor might overcount the population according to the 2000 Census in San Francisco. Such a finding might be driven by specific spatiotemporal idiosyncrasies of the San Francisco data in 2000, which is not included in the subset we analyze; however, the bulk of the literature, and all the literature which analyzes the same subset of the data we do, is consistent with our finding that Infutor undercounts the data. Diamond et al. [5] also suggest that Infutor might overcount populations due to lacking information about deaths; this is consistent with our finding that Infutor overcounts the older populations in Figure 3c.

In Figure 3, we also assess whether under- or over-represents demographic subpopulations⁸. Ramiller et al. [35] similarly study representation biases of Infutor in King County, Washington, during the 2015-2019 5-year period. They find that Infutor undercounts the county population while overrepresenting White, older, home-owning, and high-income populations. Later, they regress population errors in tract-level demographics to find that Infutor records are overrepresented in areas with higher White and high-income populations among other characteristics. We confirm most of their findings in this limited spatiotemporal scale at national level. However, the authors use the NARC3 dataset—a subset of Infutor’s address records that contains detailed demographic information—and thus, beyond the spatiotemporal scope, our analyses might be substantially different.

A.4 Assessment of additional demographic biases

We documented biases in the Infutor dataset geographically (Figure 3a) and along the dimensions of urbanization, age, race, household tenure, and poverty (Figure 3c). Here, we provide additional analyses of demographic bias by sex, educational attainment, number of children per household, and country of birth (Supplementary Figure A2). We find that Infutor displays negligible bias on the basis of sex. However, Infutor underrepresents populations with less formal education while overrepresenting populations with more formal education. Populations living in households with no children are overrepresented while those in households with children are underrepresented. This finding is consistent with the Infutor data documentation, which describes a lack of records for people under the age of 18 (therefore, children will be undercounted). Infutor also undercounts foreign-born residents by about 12%. MIGRATE essentially eliminates biases along all these demographic dimensions.

⁸Prior to conducting this assessment, we scale the Infutor population to match the overall population, so any discrepancies are not caused merely by overall undercounting

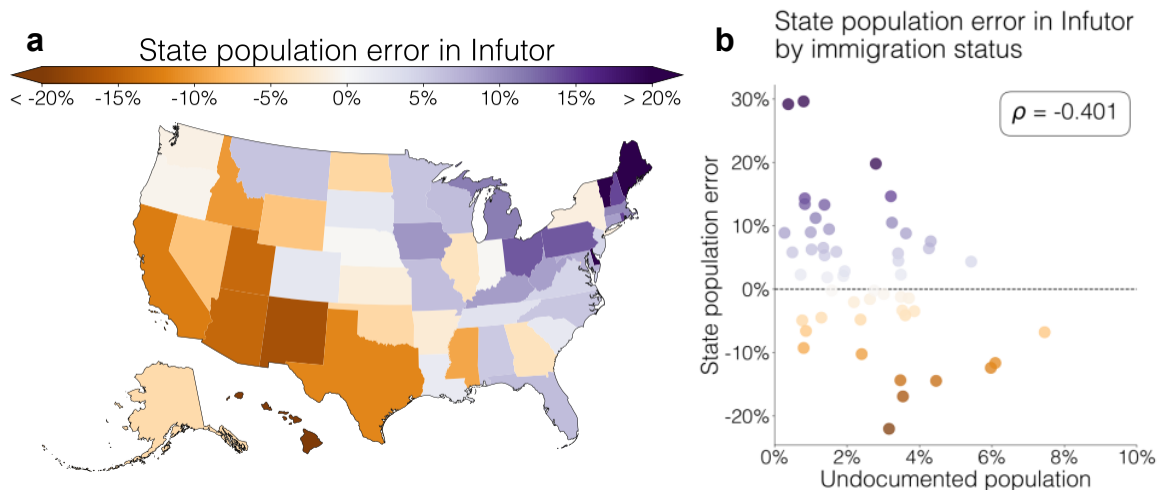


Supplementary Fig. A2: Additional analysis of socioeconomic and demographic biases at CBG population level. Variables are taken from the 5-year ACS CBG estimates. Bias is averaged over $n = 5$ population data releases (American Community Survey 5-year estimates, 2015 through 2018) Error bars represent standard deviations across these releases.

Biases in Representation of Immigrant Populations

Because of our finding that Infutor undercounts the foreign-born population, and previous research hypothesizing that Infutor may undercount undocumented immigrants specifically [13,30,92], we conduct further analyses investigating Infutor’s representation of undocumented immigrants. Infutor draws from many data sources — including cell phone bills, phone books, credit header files, public government records, property deeds, county property records, vehicle warranties, and data from vehicle repair and maintenance providers [27–29] — and some of these sources may contain data for undocumented immigrants. There were an estimated 11 million undocumented immigrants in the United States in the 2018-2022 period, about 27% of the estimated foreign-born population [93].

To measure the biases of Infutor in representing the undocumented immigrant population, we investigate whether the relative population error correlates with estimates of the undocumented population. We use data on the yearly undocumented population per state provided by the Pew Research Center [94], which is the most granular data available. As expected from the results in Figure 3a, which documents bias in Infutor data at the county level, there is geographic bias in the Infutor data at the state level as well. Infutor undercounts the population in states with larger proportions of undocumented immigrants: there is a Spearman correlation of $\rho = -0.401$ between the state-level Infutor error and the proportion of undocumented immigrants per state, averaging across the decade (Supplementary Figure A3b).



Supplementary Fig. A3: Infutor undercounts the undocumented immigrant population.

We study the representation of the undocumented immigrant population by Infutor at the state level. (a) Average errors in state populations in Infutor data relative to Census data. MIGRATE estimates remove all state-level errors by construction. (b) Spearman correlation between the estimated share of undocumented immigrants in the state population (x-axis) and error in Infutor population estimates (y-axis). Infutor is more likely to undercount states with larger proportions of undocumented immigrants.

Importantly, as with other demographic biases in the Infutor dataset, harmonizing the dataset with Census data reduces biases with respect to immigrant populations as well. Census statistics do include undocumented immigrants^[95], and so rescaling to match Census populations will mitigate Infutor’s biases.⁹ In particular, MIGRATE corrects all bias at state level by construction. As shown in Supplementary Figure A2, MIGRATE also significantly reduces the bias for the overall foreign-born population.

⁹However, Census data may also be imperfect with respect to its coverage of undocumented migrants if they are, for example, less likely to respond to surveys.

Appendix B Additional analyses of national migration

In this section we provide additional analyses of national migration trends to complement the findings of Section 4.

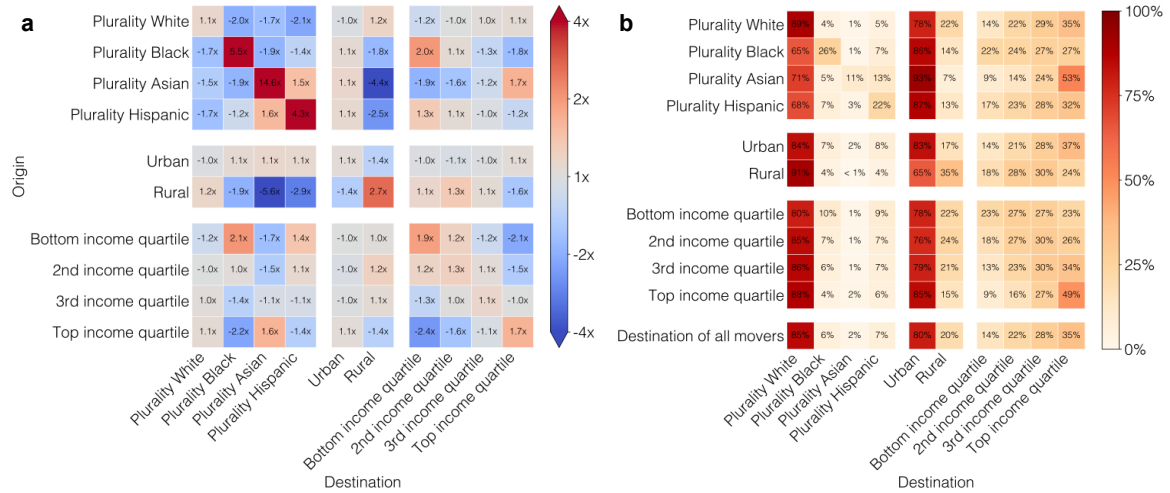
B.1 Out-migration rates by CBG type

		Out-migration rate (per 1,000)	Out-movers
Plurality Race	White	132	31,425,400
	Black	128	3,823,677
	Asian	124	889,755
	Hispanic	118	5,289,710
Urbanization	Urban	135	35,481,142
	Rural	104	5,947,401
Income Quartile	Bottom	130	8,621,155
	2nd	130	9,944,217
	3rd	131	11,011,339
	Top	128	11,851,831

Supplementary Table B1: Stratified out-migration. Out-migration rates (per 1,000 people) and raw counts of out-movers categorized by plurality race, urbanization level, and income quartile. We average the values across all years in the period.

Supplementary Table B1 reports the average out-migration rates for each of the ten CBG groups we analyze in the main text. The average out-migration rate in all CBGs is 13.0%, with 0.9% standard deviation across years. Out-migration rates are lower in plurality Hispanic and rural CBGs; out-migration rates remain similar across income quartiles.

B.2 Additional statistics on migration homophily



Supplementary Fig. B1: Additional national migration statistics. (a) Flows between the ten types of CBGs discussed in the main text relative to the share of all movers who moved to CBGs in the particular group. Each cell reports the ratio $\frac{\text{share of movers from origin CBG group moving to destination CBG group}}{\text{share of all movers moving to destination CBG group}}$; for example, the top left value of $1.1 \times$ reports the ratio of the share of movers from plurality white CBGs who move to plurality white CBGs (90%) to the share of movers from all CBGs who move to plurality white CBGs (80%). (b) Flows between the ten types of CBGs discussed in the main text when restricting to out-of-county movers demonstrate that homophily persists for long-distance moves.

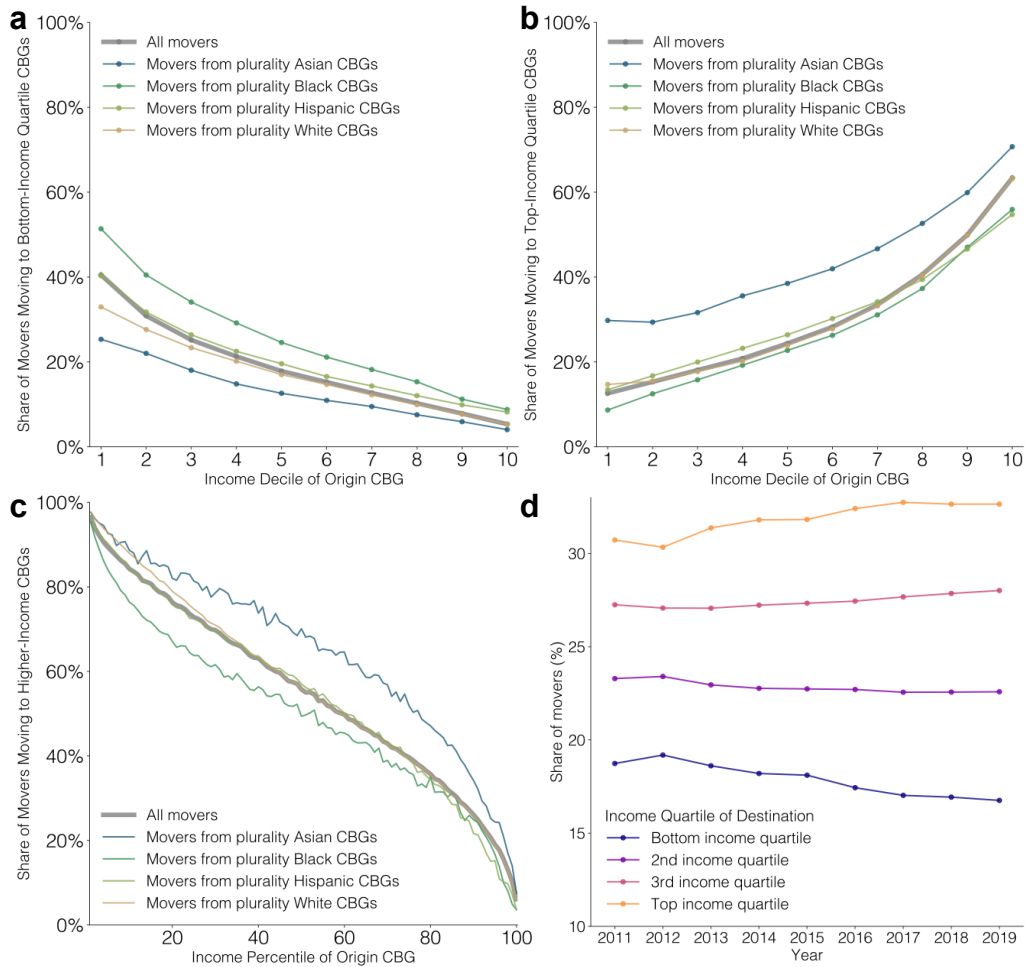
In Supplementary Figure B1, we extend the analysis of national homophily patterns in migration documented in Figure 4a. Supplementary Figure B1a shows the shares of movers moving between

groups of CBGs relative to the share of all movers who move to that group of CBGs (that is, a version of Figure 4a where the value in each cell is divided by the corresponding value in the row ‘Movers from all CBGs’).

Homophily in migration might occur because many moves are local (within county or within 5 miles) and demographics are spatially correlated. To investigate this possibility, we restrict our analysis to out-of-county moves in Figure Supplementary B1b. Absolute racial homophily is less prominent—i.e. there are smaller shares in the diagonal of the race by race submatrix—yet still present: out-of-county movers from plurality Black, Asian, and Hispanic CBGs are 4.3 \times , 5.5 \times , and 3.1 \times likelier than out-of-county movers as a whole to move to CBGs with the same plurality race group (vs. 5.5 \times , 14.6 \times , and 4.3 \times for all movers).

B.3 Additional statistics on economic mobility in migration

Supplementary Figure B2 provides additional analyses supporting our finding of racial disparities in economic mobility (Figure 4b): movers from plurality Asian CBGs are more likely than movers as a whole, and movers from plurality Black CBGs less likely, to move to higher-income CBGs, even when controlling for income of origin CBG. We show that analogous racial disparities still emerge when looking at probability of moving to a CBG in the top income quartile (Supplementary Figure B2a)



Supplementary Fig. B2: Further national migration statistics on upwards mobility. Probability of moving to a (a) top-income quartile CBG, (b) bottom-income quartile CBG, and (c) higher-income CBG conditioned on current residence median income and plurality race. In (c), we classify current residence CBGs by income percentiles as opposed to deciles (as in the main text). Disparities remain robust. (d) Movers remain more likely to move to top-income-quartile CBGs than bottom-income-quartile CBGs throughout the decade, with the disparity increasing in magnitude over time.

or bottom income quartile (Supplementary Figure B2b) as opposed to the probability of moving to a higher-income CBG (as in the main text). These disparities also emerge when controlling for origin CBG income percentile (Supplementary Figure B2c), as opposed to decile, as in the main text. We also observe that the gap in upward mobility widens during the decade: the share of movers going to a top income quartile CBG increases from 31% to 33% while the share of movers going to a bottom income quartile CBG decreases from 19% to 17% (Supplementary Figure B2d); overall, the ratio of out-movers moving to top income quartile versus bottom income quartile CBGs increases from 1.64 to 1.95.

B.4 Additional statistics on moving distance



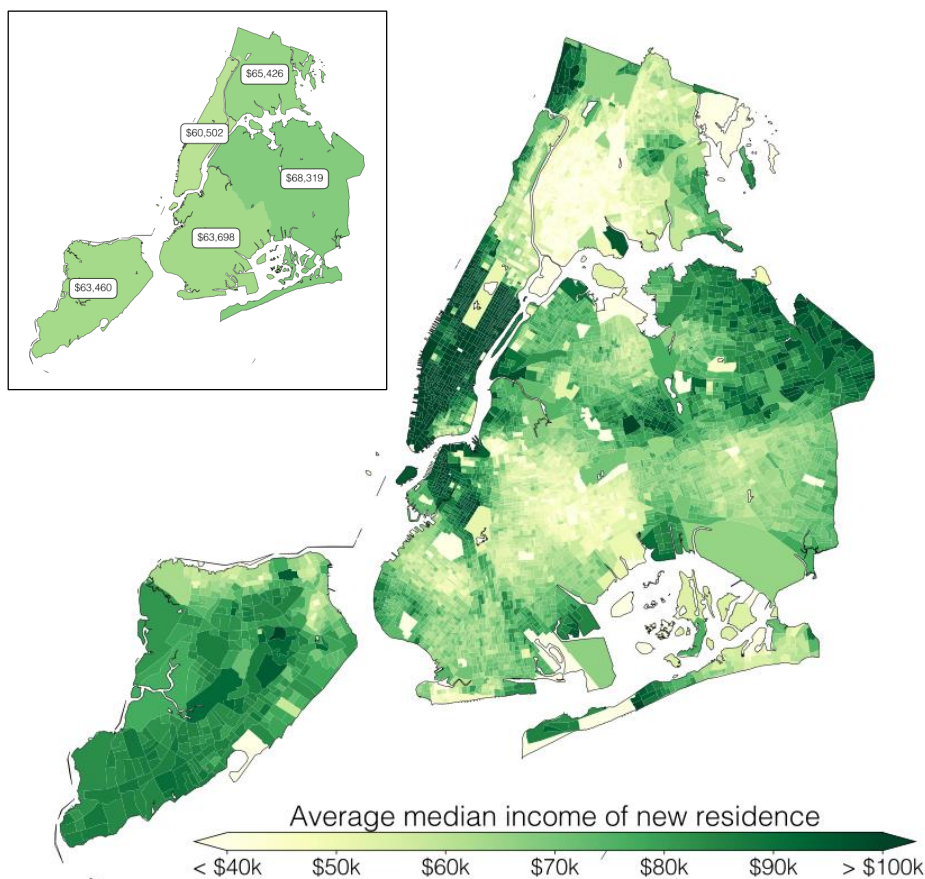
Supplementary Fig. B3: Further national migration statistics on distance moved. (a) Moving distance by year. (b) Fraction of movers moving within tract, county, and state.

Supplementary Figure B3 provides additional statistics on moving distance, expanding the findings in Figure 4c. Supplementary Figure B3a reports how moving distance changes over time, showing a general increase over the decade: the share of movers moving over 50 miles, for example, grows from about 22% to about 26%, and the average moving distance increases from 154 to 191 miles in the decade. Supplementary Figure B3b reports moving distance stratified by geographic boundary (that is, the share of movers remaining within tract, county, and state). Findings are generally consistent with those reported in Figure 4c, and also with published ACS figures, which state that over half of moves happen within counties^[25].

Appendix C Additional case studies of local migration patterns

In this section we provide two case studies of how MIGRATE reveals policy-relevant local migration patterns absent from publicly available data in New York City: a study of socioeconomic disparities on out-mover destinations, and a description of migration patterns to and from public housing buildings.

C.1 Destinations of New York City outmovers



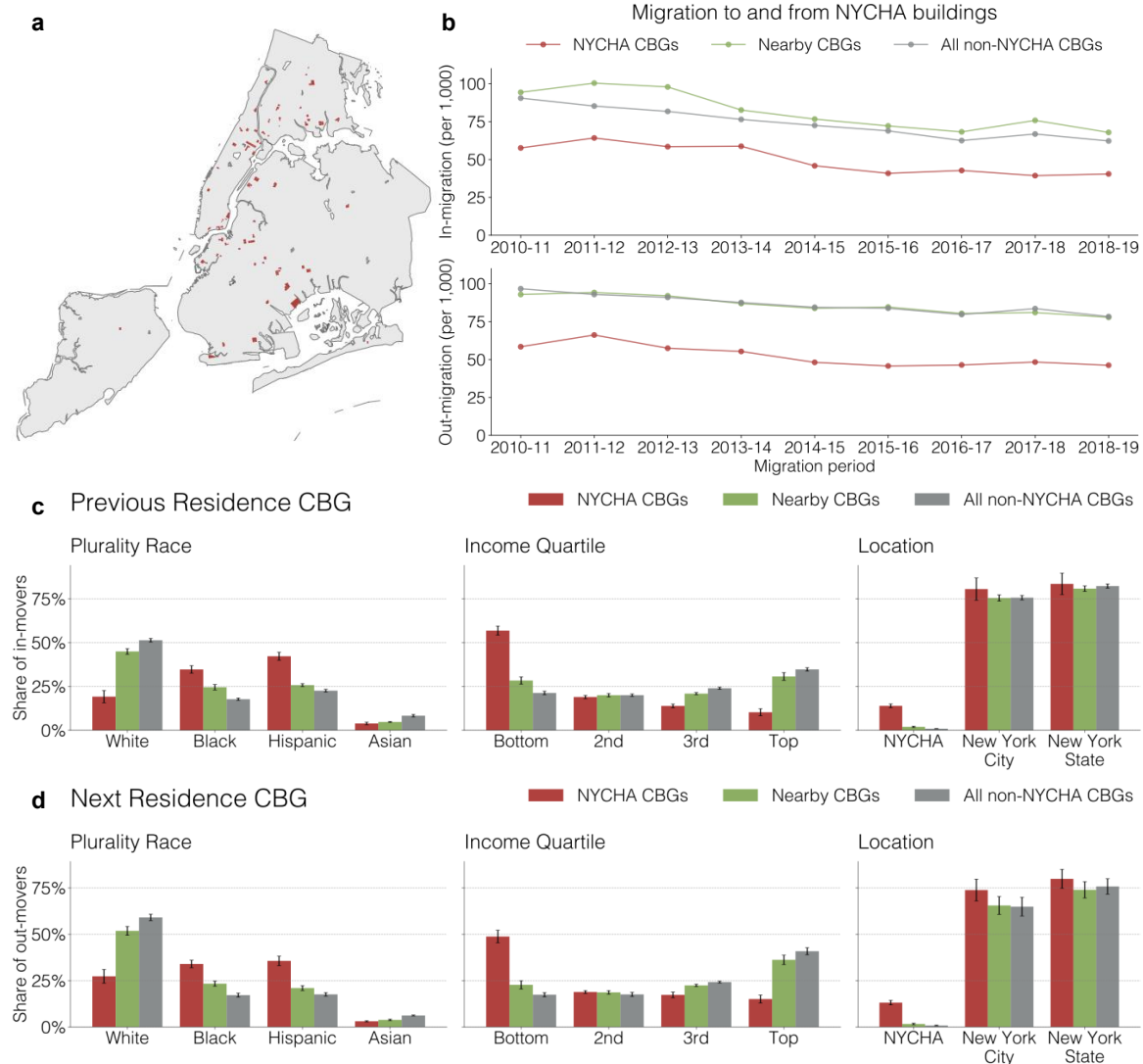
Supplementary Fig. C1: Average income (in US dollars \$) of destination CBGs and counties for New York City out-movers in the 2010-19 period. The large map uses MIGRATE estimates and 5-year ACS CBG data. The inset map shows the corresponding distribution using only publicly available migration data from 5-year ACS county-to-county estimates.

We provide a case study contrasting MIGRATE with publicly available county-to-county migration data when analyzing migration stratified by a demographic or socioeconomic feature. Supplementary Figure C1 plots the average income of the CBG to which a person moves according to their previous CBG of residence. To compute this quantity for a given CBG i , we average the mean income of all destination CBGs j for out-movers of CBG i weighted by the number of out-movers from i to j . We perform an analogous computation for the county plot in the inset.

Comparing these results to the data available at county level reveals striking within-county variation. For example, the average income of the county to which people from Manhattan moved was \$82,934—lower than that of the other four counties in New York City. MIGRATE reveals, however, that movers from some CBGs in Manhattan moved to areas with the highest average income among all New York City CBGs — above \$175,000 at times — while movers from other Manhattan CBGs moved to areas with some of the lowest average incomes. Intra-county socioeconomic differences factor heavily in out-migration: Manhattan out-movers with the highest-income destinations tended to

reside in the central and lower parts of the county (which tend to have higher incomes), whereas those with lower-income destinations came mostly from northern CBGs (which tend to have lower incomes). Similar within-county dynamics occur in the other four counties. Overall, this analysis illustrates the important demographic heterogeneity in migration which is concealed at the county level.

C.2 New York City Housing Authority



Supplementary Fig. C2: We use MIGRATE to understand migration to and from New York City Housing Authority (NYCHA) developments. **(a)** A map of the 114 Census Block Groups (marked in red) where all residential units are owned by NYCHA (i.e., where all the population lives in a NYCHA development). **(b)** Time series of in- and out-migration rates for NYCHA CBGs (red line), as well as for CBGs nearby (within 250 meters of a NYCHA development; green line) and non-NYCHA CBGs within New York City (gray line). NYCHA CBGs have consistently lower in- and out-migration rates, implying a less mobile population. **(c)** Demographics of previous residence CBG for in-movers into NYCHA buildings as well as for the other CBG groups considered, aggregated across the decade (error bars represent standard deviation across years). **(d)** Demographics of next residence CBG for out-movers.

Ensuring that residents have access to affordable housing is an important and challenging policy goal^[96]. One way of achieving this is through the creation and management of public housing units:

for example, the New York City Housing Authority (NYCHA) is the largest public housing authority in the US, providing affordable housing to over 500,000 authorized residents^[97]. We provide a case study illustrating how the MIGRATE dataset can be used to understand which residents make use of public housing units, thereby illuminating the effect of this component of affordable housing policy.

We identify all 114 New York City Census Block Groups whose residential units are entirely owned by NYCHA using New York City’s Primary Land Use Tax Lot Output (PLUTO) dataset^[98] (Supplementary Figure C2a). We compare migration patterns for these CBGs, which we refer to as “NYCHA CBGs”, to migration patterns of two other groups of non-NYCHA CBGs: (i) nearby CBGs (within 250 meters of a NYCHA development) and (ii) all non-NYCHA CBGs in New York City.¹⁰ NYCHA CBGs have had consistently lower in-migration and out-migration rates than the two comparison groups of CBGs throughout the decade (Supplementary Figure C2b), implying a less mobile population. This is consistent with prior findings that residents of public housing and recipients of rental benefits have longer tenancies than average New York City residents^[97,99].

To get a sense of the residents being served by NYCHA and their migration trajectories, we examine the demographics of the CBGs where NYCHA in-movers move from (Supplementary Figure C2c) and where NYCHA out-movers move to (Supplementary Figure C2d). Compared to non-NYCHA in-movers, NYCHA in-movers are likelier to move from plurality Black or Hispanic CBGs, as well as bottom income quartile CBGs. The same is true of NYCHA out-movers: they are also more likely to move to plurality Black or Hispanic CBGs, and bottom-income-quartile CBGs, than are non-NYCHA out-movers. The CBGs that NYCHA movers move to are higher-income than the CBGs they move from, providing evidence of upward mobility. NYCHA out-movers are also more upwardly mobile than non-NYCHA movers: 82% of NYCHA out-movers move to CBGs of higher median income, compared to 55% of all non-NYCHA out-movers.

We also quantify whether NYCHA in-movers and out-movers move within NYCHA, within New York City, and within New York State. There is a significant amount of shuffling within the NYCHA system: 14% of in-movers to a NYCHA CBG came from another NYCHA CBG, and 13% of out-movers from a NYCHA building go to another NYCHA CBG. This shuffling may be due in part to mandated renovations or building closures that result in temporary resident relocations by NYCHA^[100–102]. On average across the decade that we study, NYCHA out-movers are likelier than non-NYCHA movers to remain within New York City (74% vs. 65%); however, this gap has decreased in recent years.

Overall, this analysis highlights how MIGRATE can provide insights into which residents are served by public housing policy. Beyond this case study of New York City, this approach could be extended to study public housing in other cities, or to study the effects of public housing foreclosures—which has been a topic of interest among other migration researchers^[13].

¹⁰We excluded from the analysis all 345 CBGs (about 5.3% of all New York City CBGs) where some but not all of the residential units are owned by NYCHA.

Appendix D Privacy Protections

In this section we detail the measures we took to preserve the privacy of individuals in the MIGRATE data release. Analysis of the Infutor dataset was determined to be not human subjects research by the Cornell Institutional Review Board (IRB #0145225).

First, in contrast to the original Infutor data, the data we release is aggregated: it contains only estimated migration between CBG-CBG pairs, and no information about individuals. This level of data aggregation is consistent with other data sources which have been made available to researchers. For example, mobility data often contains the aggregate counts of individuals moving from a given CBG to a given point of interest on a given day^[40,103–106].

Second, the matrices we release are probabilistic and rescaled: in particular, the fact that a particular entry of the CBG-CBG migration matrix is non-zero does not guarantee that a given number of individuals moved between those CBGs (or indeed, that any did at all). This is because individuals are mapped probabilistically to CBGs (e.g., if we have only a ZIP code for an individual, they are mapped probabilistically to CBGs within that ZIP code) and the migration matrices are rescaled multiple times.

Third, we release the data only to researchers for non-profit use who agree to a data use agreement pledging not to re-identify individuals in the data, and to adhere to privacy-protecting measures when storing data and presenting results, following manual review of their application and research project.

Finally, we compute the average number of destinations (unique CBGs) for out-movers from each CBG. The purpose of the analysis is to assess how difficult it would be to track a given individual if one knew they lived in a given CBG and then moved. Across CBGs and years, the mean number of destinations for outmovers is 272.2 (median 234). We redact from the public data release migration information for the very small proportion of CBGs (0.558%) for which 90% of out-movers travel to 10 or fewer CBGs. All analyses in the paper were conducted with the full data.

References

- [1] Hoffmann, R., Abel, G., Malpede, M., Muttarak, R., Percoco, M.: Drought and aridity influence internal migration worldwide. *Nature Climate Change* **14**(12), 1245–1253 (2024) <https://doi.org/10.1038/s41558-024-02165-1> . Publisher: Nature Publishing Group. Accessed 2025-01-24
- [2] Kaysen, R.: Open Houses in Los Angeles Take on an Eerie Feeling. *The New York Times* (2025). Chap. Real Estate. Accessed 2025-01-24
- [3] McConnell, K., Fussell, E., DeWaard, J., Whitaker, S., Curtis, K.J., St. Denis, L., Balch, J., Price, K.: Rare and highly destructive wildfires drive human migration in the U.S. *Nature Communications* **15**(1), 6631 (2024) <https://doi.org/10.1038/s41467-024-50630-4> . Publisher: Nature Publishing Group. Accessed 2025-01-24
- [4] Alexander, M., Polimis, K., Zagheni, E.: The impact of hurricane maria on out-migration from puerto rico: Evidence from facebook data. *Population and Development Review*, 617–630 (2019)
- [5] Diamond, R., Guren, A., Tan, R.: The Effect of Foreclosures on Homeowners, Tenants, and Landlords. National Bureau of Economic Research (2020). <https://doi.org/10.3386/w27358> . <https://www.nber.org/papers/w27358> Accessed 2025-01-24
- [6] Wilkerson, I.: *The Warmth of Other Suns: The Epic Story of America’s Great Migration*. Knopf, New York (2010)
- [7] Niva, V., Horton, A., Virkki, V., Heino, M., Kosonen, M., Kallio, M., Kinnunen, P., Abel, G.J., Muttarak, R., Taka, M., Varis, O., Kumm, M.: World’s human migration patterns in 2000–2019 unveiled by high-resolution data. *Nature Human Behaviour* **7**(11), 2023–2037 (2023) <https://doi.org/10.1038/s41562-023-01689-4> . Publisher: Nature Publishing Group. Accessed 2025-01-24
- [8] Boucherie, L., Maier, B.F., Lehmann, S.: Decoupling geographical constraints from human mobility. *Nature Human Behaviour* (2025) <https://doi.org/10.1038/s41562-025-02282-7>
- [9] DePillis, L.: For L.G.B.T.Q. People, Moving to Friendlier States Comes With a Cost. *The New York Times* (2024). Chap. Business. Accessed 2025-01-24
- [10] Chi, G., Abel, G.J., Johnston, D., Giraudy, E., Bailey, M.: Measuring global migration flows using online data. *Proceedings of the National Academy of Sciences* **122**(18), 2409418122 (2025) <https://doi.org/10.1073/pnas.2409418122> <https://www.pnas.org/doi/pdf/10.1073/pnas.2409418122>
- [11] Leasure, D.R., Kashyap, R., Rampazzo, F., Dooley, C.A., Elbers, B., Bondarenko, M., Verhagen, M., Frey, A., Yan, J., Akimova, E.T., *et al.*: Nowcasting daily population displacement in ukraine through social media advertising data. *Population and Development Review* **49**(2), 231–254 (2023)
- [12] Ramani, A., Alcedo, J., Bloom, N.: How working from home reshapes cities. *Proceedings of the National Academy of Sciences* **121**(45), 2408930121 (2024) <https://doi.org/10.1073/pnas.2408930121> . Company: National Academy of Sciences Distributor: National Academy of Sciences Institution: National Academy of Sciences Label: National Academy of Sciences Publisher: Proceedings of the National Academy of Sciences. Accessed 2025-01-24
- [13] Phillips, D.C.: Measuring Housing Stability With Consumer Reference Data. *Demography* **57**(4), 1323–1344 (2020) <https://doi.org/10.1007/s13524-020-00893-5>
- [14] Gershenson, C., Jin, O., Haas, J., Desmond, M.: Fracking evictions: Housing instability in a fossil fuel boomtown. *Society & Natural Resources* **37**(3), 347–364 (2024)

- [15] Golding, S.A., Winkler, R.L.: Tracking urbanization and exurbs: Migration across the rural–urban continuum, 1990–2016. *Population research and policy review* **39**(5), 835–859 (2020)
- [16] Reia, S.M., Rao, P.S.C., Barthelemy, M., Ukkusuri, S.V.: Spatial structure of city population growth. *Nature communications* **13**(1), 5931 (2022)
- [17] Kaysen, R., Singer, E.: Millions of Movers Reveal American Polarization in Action. *The New York Times* (2024). Chap. The Upshot. Accessed 2025-01-24
- [18] U.S. Census Bureau: County-to-County Migration Flows. Section: Government (2024). <https://www.census.gov/topics/population/migration/guidance/county-to-county-migration-flows.html> Accessed 2025-05-14
- [19] Shu, E.G., Porter, J.R., Hauer, M.E., Sandoval Olascoaga, S., Gourevitch, J., Wilson, B., Pope, M., Melecio-Vazquez, D., Kearns, E.: Integrating climate change induced flood risk into future population projections. *Nature Communications* **14**(1), 7870 (2023)
- [20] Craig, D.G.: America’s great climate migration has begun. here’s what you need to know. *Columbia Magazine* (2024). Accessed: 2024-12-05
- [21] Tedesco, M., Hultquist, C., Char, S.E., Constantinides, C., Galjanic, T., Sinha, A.D.: Socio-Economic, Physical, Housing, Eviction, and Risk dataset, version 2 (SEPPER 2.0), Preliminary Release (2021). <https://doi.org/10.7927/r6yw-xw73>
- [22] Rising, J., Tedesco, M., Piontek, F., Stainforth, D.A.: The missing risks of climate change. *Nature* **610**(7933), 643–651 (2022)
- [23] Freedman, A.A., Smart, B.P., Keenan-Devlin, L.S., Borders, A., Ernst, L.M., Miller, G.E.: Living in a block group with a higher eviction rate is associated with increased odds of preterm delivery. *Journal of epidemiology and community health* **76**(4), 398–403 (2022) <https://doi.org/10.1136/jech-2020-215377> . Accessed 2025-08-12
- [24] Rutan, D.Q., Desmond, M.: The Concentrated Geography of Eviction. *The ANNALS of the American Academy of Political and Social Science* **693**(1), 64–81 (2021) <https://doi.org/10.1177/0002716221991458> . Publisher: SAGE Publications Inc. Accessed 2025-08-12
- [25] Kerns-D’Amore, K., McKenzie, B., Locklear, L.S.: Migration in the United States: 2006 to 2019. Technical Report ACS-53, American Community Survey (July 2023). <https://www.census.gov/content/dam/Census/library/publications/2023/acs/acs-53.pdf>
- [26] Infutor Data Solutions, LLC: Infutor Data Solutions - Batch Documentation (2019). <https://batchdocs.infutor.com/> Accessed 2025-03-20
- [27] Diamond, R., McQuade, T., Qian, F.: The Effects of Rent Control Expansion on Tenants, Landlords, and Inequality: Evidence from San Francisco. *American Economic Review* **109**(9), 3365–3394 (2019) <https://doi.org/10.1257/aer.20181289> . Accessed 2025-01-24
- [28] Phillips, D.C., Sullivan, J.X.: Personalizing homelessness prevention: Evidence from a randomized controlled trial. *Journal of Policy Analysis and Management* **43**(4), 1101–1128 (2024) <https://doi.org/10.1002/pam.22547> <https://onlinelibrary.wiley.com/doi/pdf/10.1002/pam.22547>
- [29] Boar, C., Giannone, E.: Consumption segregation. Technical report, National Bureau of Economic Research (2023)
- [30] Bernstein, S., Diamond, R., Jiranaphawiboon, A., McQuade, T., Pousada, B.: The contribution of high-skilled immigrants to innovation in the united states. Technical report, National Bureau of Economic Research (2022)
- [31] Asquith, B., Mast, E., Reed, D.: Supply shock versus demand shock: The local effects of new housing in low-income areas. Available at SSRN 3507532 (2019)

- [32] Qian, F., Tan, R.: The effects of high-skilled firm entry on incumbent residents. Stanford Institute for Economic Policy Research (SIEPR) Working Paper, 21–039 (2021)
- [33] Alexander, M., Polimis, K., Zagheni, E.: Combining social media and survey data to nowcast migrant stocks in the united states. *Population Research and Policy Review* **41**(1), 1–28 (2022)
- [34] Rampazzo, F., Bijak, J., Vitali, A., Weber, I., Zagheni, E.: Assessing timely migration trends through digital traces: a case study of the uk before brexit. *International Migration Review* **59**(1), 119–140 (2025)
- [35] Ramiller, A., Song, T., Parker, M., Chapple, K.: Residential Mobility and Big Data: Assessing the Validity of Consumer Reference Datasets. *Cityscape* **26**(3), 227–240 (2024). Publisher: US Department of Housing and Urban Development. Accessed 2025-01-24
- [36] Imbens, G.W., Lancaster, T.: Combining Micro and Macro Data in Microeconomic Models. *The Review of Economic Studies* **61**(4), 655–680 (1994) <https://doi.org/10.2307/2297913> . Accessed 2025-09-03
- [37] Guan, A., Reitsma, M., Sahoo, R., Salomon, J., Wager, S.: Data Fusion for High-Resolution Estimation (2025). <https://arxiv.org/abs/2508.14858>
- [38] Deming, W.E., Stephan, F.F.: On a Least Squares Adjustment of a Sampled Frequency Table When the Expected Marginal Totals are Known. *The Annals of Mathematical Statistics* **11**(4), 427–444 (1940) <https://doi.org/10.1214/aoms/1177731829>
- [39] Chang, S., Koehler, F., Qu, Z., Leskovec, J., Ugander, J.: Inferring dynamic networks from marginals with iterative proportional fitting. *ICML* (2024)
- [40] Chang, S., Pierson, E., Koh, P.W., Gerardin, J., Redbird, B., Grusky, D., Leskovec, J.: Mobility network models of covid-19 explain inequities and inform reopening. *Nature* **589**(7840), 82–87 (2021)
- [41] Dong, E., Schein, A., Wang, Y., Garg, N.: Addressing discretization-induced bias in demographic prediction. *PNAS Nexus* **4**(2), 027 (2025) <https://doi.org/10.1093/pnasnexus/pgaf027> <https://academic.oup.com/pnasnexus/article-pdf/4/2/pgaf027/61698986/pgaf027.pdf>
- [42] Hernangómez, D.: arcgeocoder: Geocoding with the ArcGIS REST API Service. (2024). <https://doi.org/10.32614/CRAN.package.arcgeocoder> . <https://dieghernan.github.io/arcgeocoder/>
- [43] U.S. Census Bureau: Census Geocoder User Guide. U.S. Government Publishing Office (2024). https://www2.census.gov/geo/pdfs/maps-data/data/Census_Geocoder_User_Guide.pdf
- [44] Hastie, T., Tibshirani, R., Friedman, J.: *The Elements of Statistical Learning: Data Mining, Inference, and Prediction*, 2nd edn. Springer, New York (2009). 2nd edition. <https://hastie.su.domains/ElemStatLearn/>
- [45] McConnell, K., Whitaker, S., Fussell, E., DeWaard, J., Price, K., Curtis, K.: Effects of wildfire destruction on migration, consumer credit, and financial distress. FRB of Cleveland Working Paper (2021)
- [46] Modaresi Rad, A., Abatzoglou, J.T., Kreitler, J., Alizadeh, M.R., AghaKouchak, A., Hudyma, N., Nauslar, N.J., Sadegh, M.: Human and infrastructure exposure to large wildfires in the United States. *Nature Sustainability* **6**(11), 1343–1351 (2023) <https://doi.org/10.1038/s41893-023-01163-z> . Publisher: Nature Publishing Group. Accessed 2025-02-27
- [47] Barbero, R., Abatzoglou, J.T., Larkin, N.K., Kolden, C.A., Stocks, B.: Climate change presents increased potential for very large fires in the contiguous united states. *International Journal of Wildland Fire* **24**(7), 892 (2015) <https://doi.org/10.1071/wf15083>
- [48] Din, A.: Graphic Detail: What Do Visualizations of Administrative Address Data Show About

the Camp Fire. *Cityscape: A Journal of Policy Development and Research* (2022)

- [49] Rosenthal, A., Stover, E., Haar, R.J.: Health and social impacts of california wildfires and the deficiencies in current recovery resources: An exploratory qualitative study of systems-level issues. *PloS one* **16**(3), 0248617 (2021)
- [50] Hopfer, S., Jiao, A., Li, M., Vargas, A.L., Wu, J.: Repeat wildfire and smoke experiences shared by four communities in southern california: local impacts and community needs. *Environmental Research: Health* **2**(3), 035013 (2024)
- [51] Isaac, F., Toukhsati, S.R., Klein, B., Di Benedetto, M., Kennedy, G.A.: Differences in anxiety, insomnia, and trauma symptoms in wildfire survivors from australia, canada, and the united states of america. *International Journal of Environmental Research and Public Health* **21**(1), 38 (2023)
- [52] McWethy, D.B., Schoennagel, T., Higuera, P.E., Krawchuk, M., Harvey, B.J., Metcalf, E.C., Schultz, C., Miller, C., Metcalf, A.L., Buma, B., *et al.*: Rethinking resilience to wildfire. *Nature Sustainability* **2**(9), 797–804 (2019)
- [53] Mach, K.J., Siders, A.: Reframing strategic, managed retreat for transformative climate adaptation. *Science* **372**(6548), 1294–1299 (2021)
- [54] Boomhower, J., Fowlie, M., Gellman, J., Plantinga, A.: How Are Insurance Markets Adapting to Climate Change? Risk Classification and Pricing in the Market for Homeowners Insurance. Technical Report w32625, National Bureau of Economic Research, Cambridge, MA (June 2024). <https://doi.org/10.3386/w32625> . <http://www.nber.org/papers/w32625.pdf> Accessed 2025-02-27
- [55] Patrick Baylis, J.B.: Mandated vs. voluntary adaptation to natural disasters: The case of u.s. wildfires. Technical Report w29621, National Bureau of Economic Research, Cambridge, MA (dec 2021). https://www.nber.org/system/files/working_papers/w29621/w29621.pdf Accessed 2025-02-27
- [56] Kramer, H.A., Butsic, V., Mockrin, M.H., Ramirez-Reyes, C., Alexandre, P.M., Radeloff, V.C.: Post-wildfire rebuilding and new development in California indicates minimal adaptation to fire risk. *Land Use Policy* **107**, 105502 (2021) <https://doi.org/10.1016/j.landusepol.2021.105502> . Accessed 2025-02-27
- [57] Alexandre, P.M., Mockrin, M.H., Stewart, S.I., Hammer, R.B., Radeloff, V.C.: Rebuilding and new housing development after wildfire. *International Journal of Wildland Fire* **24**(1), 138–149 (2014) <https://doi.org/10.1071/WF13197> . Publisher: CSIRO PUBLISHING. Accessed 2025-02-27
- [58] Lee, J., Costa, R., Baker, J.W.: Post-disaster housing recovery estimation: Data and lessons learned from the 2017 Tubbs and 2018 Camp Fires. *International Journal of Disaster Risk Reduction* **114**, 104912 (2024) <https://doi.org/10.1016/j.ijdr.2024.104912> . Accessed 2025-02-27
- [59] Bohra-Mishra, P., Oppenheimer, M., Hsiang, S.M.: Nonlinear permanent migration response to climatic variations but minimal response to disasters. *Proceedings of the National Academy of Sciences* **111**(27), 9780–9785 (2014)
- [60] Cattaneo, C., Peri, G.: The migration response to increasing temperatures. *Journal of Development Economics* **122**, 127–146 (2016)
- [61] Benveniste, H., Huybers, P., Proctor, J.: Global Climate Migration is a Story of Who, Not Just How Many. Available at SSRN: <https://ssrn.com/abstract=4925994> (2024). <https://doi.org/10.2139/ssrn.4925994>
- [62] Hino, M., Field, C.B., Mach, K.J.: Managed retreat as a response to natural hazard risk. *Nature*

Climate Change **7**(5), 364–370 (2017)

- [63] California Department of Forestry and Fire Protection: Historical Fire Perimeters (2024). <https://www.fire.ca.gov/what-we-do/fire-resource-assessment-program/fire-perimeters> Accessed 2025-03-14
- [64] California Department of Forestry and Fire Protection: Tubbs Fire (Central LNU Complex) (2025). <https://www.fire.ca.gov/incidents/2017/10/8/tubbs-fire-central-lnu-complex> Accessed 2025-03-14
- [65] California Department of Forestry and Fire Protection: Camp Fire (2025). <https://www.fire.ca.gov/incidents/2018/11/8/camp-fire/> Accessed 2025-03-14
- [66] California Department of Forestry and Fire Protection: Top 20 Most Destructive California Wildfires (2025). <https://www.fire.ca.gov/our-impact/statistics> Accessed 2025-03-14
- [67] Quillian, L.: Why is black–white residential segregation so persistent?: Evidence on three theories from migration data. *Social Science Research* **31**(2), 197–229 (2002)
- [68] Boustan, L.P.: Racial residential segregation in american cities. Technical report, National Bureau of Economic Research (2013)
- [69] Dawkins, C.J.: Recent evidence on the continuing causes of black-white residential segregation. *Journal of Urban Affairs* **26**(3), 379–400 (2004)
- [70] South, S.J., Pais, J., Crowder, K.: Metropolitan influences on migration into poor and nonpoor neighborhoods. *Social Science Research* **40**(3), 950–964 (2011)
- [71] Pais, J., South, S.J., Crowder, K.: Metropolitan heterogeneity and minority neighborhood attainment: Spatial assimilation or place stratification? *Social problems* **59**(2), 258–281 (2012)
- [72] South, S.J., Huang, Y., Spring, A., Crowder, K.: Neighborhood attainment over the adult life course. *American Sociological Review* **81**(6), 1276–1304 (2016)
- [73] Quillian, L.: A comparison of traditional and discrete-choice approaches to the analysis of residential mobility and locational attainment. *The ANNALS of the American Academy of Political and Social Science* **660**(1), 240–260 (2015)
- [74] Fraga, B.L., Holbein, J.B., Skovron, C.: Using nationwide voter files to study the effects of election laws. Technical report, Working Paper, University of Virginia (2018)
- [75] Kim, S.-y.S., Fraga, B.: When Do Voter Files Accurately Measure Turnout? How Transitory Voter File Snapshots Impact Research and Representation. APSA Preprints (2022). <https://doi.org/10.33774/apsa-2022-qr0gd> . <https://preprints.apsanet.org/engage/apsa/article-details/6321ef75faf4a4ba6f1213ef> Accessed 2025-03-20
- [76] Wilson, R., Din, A.: Understanding and Enhancing the U.S. Department of Housing and Urban Development’s ZIP Code Crosswalk Files. *Cityscape* **20**(2), 277–294 (2018)
- [77] U.S. Census Bureau: 2024 ACS and PRCS Design and Methodology Version 4.0. U.S. Government Publishing Office (2024). https://www2.census.gov/programs-surveys/acs/methodology/design_and_methodology/2024/acs_design_methodology_report_2024.pdf
- [78] U.S. Census Bureau: Substantial Changes to Counties and County Equivalent Entities: 1970–Present. Section: Government (2021). <https://www.census.gov/programs-surveys/geography/technical-documentation/county-changes.html> Accessed 2025-03-19
- [79] U.S. Census Bureau: 2011 Geography Changes. Section: Government (2021). <https://www.census.gov/programs-surveys/acs/technical-documentation/table-and-geography-changes/2011/geography-changes.html> Accessed 2025-03-19

- [80] U.S. Census Bureau: Understanding and Using American Community Survey Data: What All Data Users Need to Know. U.S. Government Publishing Office (2020)
- [81] Schroeder, J., Van Riper, D., Manson, S., Knowles, K., Kugler, T., Roberts, F., Ruggles, S.: IPUMS National Historical Geographic Information System: Version 20.0. IPUMS, Minneapolis, MN. [dataset] (2025). <https://doi.org/10.18128/D050.V20.0> . <http://doi.org/10.18128/D050.V20.0>
- [82] U.S. Census Bureau: American Community Survey Migration Flows [dataset]. <https://www.census.gov/data/developers/data-sets/acs-migration-flows.html>. Accessed September 2025 (2024)
- [83] U.S. Census Bureau: Population and Housing Unit Estimates. Section: Government (2025). <https://www.census.gov/popest> Accessed 2025-03-15
- [84] Lautz, J.: Long-distance Movers: Why Did They Move and How? (2023). <https://www.nar.realtor/blogs/economists-outlook/long-distance-movers-why-did-they-move-and-how> Accessed 2025-03-20
- [85] U.S. Census Bureau: Population Controls for the 2021 ACS. Section: Government (2022). <https://www.census.gov/programs-surveys/acs/technical-documentation/user-notes/2022-10.html> Accessed 2025-03-15
- [86] Balachandar, S., Garg, N., Pierson, E.: Domain constraints improve risk prediction when outcome data is missing. In: The Twelfth International Conference on Learning Representations (2024). <https://openreview.net/forum?id=1mNFsbvo2P>
- [87] Agostini, G., Pierson, E., Garg, N.: A bayesian spatial model to correct under-reporting in urban crowdsourcing. In: Proceedings of the AAAI Conference on Artificial Intelligence, vol. 38, pp. 21888–21896 (2024)
- [88] Pierson, E., Koh, P.W., Hashimoto, T., Koller, D., Leskovec, J., Eriksson, N., Liang, P.: Inferring multidimensional rates of aging from cross-sectional data. In: The 22nd International Conference on Artificial Intelligence and Statistics, pp. 97–107 (2019). PMLR
- [89] Birkin, M., Clarke, M.: Synthesis—A Synthetic Spatial Information System for Urban and Regional Analysis: Methods and Examples. *Environment and Planning A: Economy and Space* **20**(12), 1645–1671 (1988) <https://doi.org/10.1068/a201645> . Publisher: SAGE Publications Ltd. Accessed 2025-09-03
- [90] Wong, D.W.S.: The Reliability of Using the Iterative Proportional Fitting Procedure. *The Professional Geographer* **44**(3), 340–348 (1992) <https://doi.org/10.1111/j.0033-0124.1992.00340.x> . eprint: <https://onlinelibrary.wiley.com/doi/pdf/10.1111/j.0033-0124.1992.00340.x>. Accessed 2025-09-03
- [91] Simpson, L., Tranmer, M.: Combining Sample and Census Data in Small Area Estimates: Iterative Proportional Fitting with Standard Software. *The Professional Geographer* **57**(2), 222–234 (2005) <https://doi.org/10.1111/j.0033-0124.2005.00474.x> . eprint: <https://onlinelibrary.wiley.com/doi/pdf/10.1111/j.0033-0124.2005.00474.x>. Accessed 2025-09-03
- [92] Downes, H., Zuo, G.: Can moves to opportunity be constructed? evidence from the low-income housing tax credit. In: 2023 APPAM Fall Research Conference (2023). APPAM
- [93] Baker, B., Warren, R.: Estimates of the Unauthorized Immigrant Population Residing in the United States: January 2018–January 2022. Office of Homeland Security Statistics (2024). <https://ohss.dhs.gov/topics/immigration/unauthorized/population-estimates> Accessed 2025-08-07

- [94] Passel, J., Krogstad, J.: What we know about unauthorized immigrants living in the US (2024). <https://www.pewresearch.org/short-reads/2024/07/22/what-we-know-about-unauthorized-immigrants-living-in-the-us> Accessed 2025-08-15
- [95] US Census Bureau: About the Foreign-Born Population. Section: Government (2025). <https://www.census.gov/topics/population/foreign-born/about.html> Accessed 2025-08-07
- [96] Favilukis, J., Mabile, P., Van Nieuwerburgh, S.: Affordable housing and city welfare. *The Review of Economic Studies* **90**(1), 293–330 (2023)
- [97] New York City Housing Authority: NYCHA Fact Sheet. Accessed: 2025-05-06 (2024). https://www.nyc.gov/assets/nycha/downloads/pdf/NYCHA_Fact_Sheet.pdf
- [98] New York City Department of City Planning: Primary Land Use Tax Lot Output (PLUTO). <https://www.nyc.gov/site/planning/data-maps/open-data/dwn-pluto-mappluto.page>. Accessed: 2025-05-04 (2024)
- [99] Chen, R., Jiang, H., Quintero, L.E.: Measuring the value of rent stabilization and understanding its implications for racial inequality: Evidence from New York City. *Regional Science and Urban Economics* **103**, 103948 (2023) <https://doi.org/10.1016/j.regsciurbeco.2023.103948> . Accessed 2025-05-06
- [100] Navarro, M.: Harlem Housing Relic From the 1800s Is Set for a Long-Promised Overhaul. *The New York Times* (2014). Chap. New York. Accessed 2025-05-06
- [101] Fernandez, M.: New York Plans to Topple Public Housing Towers. *The New York Times* (2010). Chap. New York. Accessed 2025-05-06
- [102] Zaveri, M.: To Improve Public Housing, New York City Moves to Tear It Down. *The New York Times* (2023). Chap. New York. Accessed 2025-05-06
- [103] Abbiasov, T., Heine, C., Sabouri, S., Salazar-Miranda, A., Santi, P., Glaeser, E., Ratti, C.: The 15-minute city quantified using human mobility data. *Nature Human Behaviour* **8**(3), 445–455 (2024)
- [104] Kostandova, N., Schluth, C., Arambepola, R., Atuhaire, F., Bérubé, S., Chin, T., Cleary, E., Cortes-Azuerro, O., García-Carreras, B., Grantz, K.H., *et al.*: A systematic review of using population-level human mobility data to understand sars-cov-2 transmission. *Nature Communications* **15**(1), 1–12 (2024)
- [105] Xu, F., Wang, Q., Moro, E., Chen, L., Salazar Miranda, A., González, M.C., Tizzoni, M., Song, C., Ratti, C., Bettencourt, L., *et al.*: Using human mobility data to quantify experienced urban inequalities. *Nature Human Behaviour*, 1–11 (2025)
- [106] Yabe, T., García Bulle Bueno, B., Frank, M.R., Pentland, A., Moro, E.: Behaviour-based dependency networks between places shape urban economic resilience. *Nature Human Behaviour*, 1–11 (2024)